Database on wind characteristics - Analyses of wind turbine design loads

Larsen, Gunner Chr.; Hansen, K.S.

Publication date:
2004

Document Version
Publisher's PDF, also known as Version of record

Risø-R-1473(EN)

Database on Wind Characteristics

Analyses of Wind Turbine Design Loads

Gunner C. Larsen and Kurt S. Hansen

Risø National Laboratory, Roskilde
June 2004

Abstract The main objective of IEA R&D Wind Annex XVII - Database on Wind

Characteristics - has been to provide wind energy planners, designers and researchers, as well as the international wind engineering community in general, with a source of actual wind field data (time series and resource data) observed in a wide range of different wind climates and terrain types. Connected to an extension of the initial Annex period, the scope for the continuation was widened to include also support to the international wind turbine standardisation efforts. The project partners are Sweden, Norway, U.S.A., The Netherlands and Denmark, with Denmark as the Operating Agent.

The reporting of the continuation of Annex XVII falls in two separate parts. Part one accounts in details for the available data in the established database bank [12], and part two describes various data analyses performed with the overall purpose of improving the design load cases with relevance for to wind turbine structures.

The present report constitutes the second part of the Annex XVII reporting. Both fatigue and extreme load aspects are dealt with, however, with the main emphasis on the latter.

IEA R&D Wind Annex XVII
Database on Wind Characteristics

http://www.winddata.com/

E-mail: winddata@mek.dtu.dk

Gunner Chr. Larsen
Wind Energy and Atmospheric
Physics Department
Risø National Laboratory
Post Office Box 49
DK-4000 Roskilde

E-mail: gunner.larsen@risoe.dk

Kurt S. Hansen
Fluid Mechanics Section
Department of Mechanical Engineering
Technical University of Denmark
Nils Koppels Allé
DTU-Building 403
DK-2800 Lyngby
E-mail: ksh@mek.dtu.dk

ISBN 87-550-3359-8 (Internet)
ISSN 0106-2840

Print: Pitney Bowes Management Services Denmark, 2004

Contents

1 Background

In 1996, the EU-DG XII (JOULE) project “Database on Wind Characteristics” was started. The project was concluded at the end of 1998 and resulted in a unique database of quality controlled and well-documented wind field measurements in a standardised format. The established data bank was supplemented with tools to enable access and simple analysis through an Internet connection using the World-Wide-Web. The contents and the facilities are reported in [1].

As a follow-up to the JOULE project, Annex XVII, within the auspices of the IEA R&D Wind, was formulated with Sweden, Norway, U.S.A., The Netherlands, Japan and Denmark as active participants. The Annex entered into force on 1st January 1999, and an initial annex period of two and a half year was successfully concluded on 30st June 2001. The main objective of Annex XVII was to provide wind energy planners and designers, as well as the international wind engineering community in general, with easy access to quality controlled measured wind field time series observed in a wide range of environments. From its inception Annex XVII has successfully met the purpose by ensuring that the database is always on-line and available through the Internet, and by making possible and managing the continuous development and dissemination of the database. The achievements, covering this initial annex period are reported in [2], [3] and [4].

With the purpose of continuing the ongoing maintenance and dissemination, accomplish the initiated extension of facilities and content, and further to support the international wind turbine standardisation efforts, IEA decided to run Annex XVII for an additional period of 2.5 years. The continuation of Annex XVII entered into force on 1st July 2001 and was concluded on 31st December 2003.

2 Introduction

The reporting of the 2.5 years continuation of Annex XVII falls in two separate parts. Part one accounts in details for the available data in the established database bank, and part two describes various data analyses performed with the overall purpose of improving and validating code specifications for wind turbine design on a rational basis.

The present report constitutes part two of the Annex XVII reporting. Of fundamental importance for development of wind turbine code specifications is the availability of a well documented and (load) representative data material. During the course of Annex XVII, "Database on Wind Characteristics" has gradually evolved to a more and more unique tool for rational calibration and improvement of design load cases, as specified in international codes, due to its content of a broad spectrum of representative wind turbine site field measurements.

Based on data extracted from "Database on Wind Characteristics", a range of design load analyses have been performed. Both fatigue, cf. [5] - [6], and extreme load, cf. [7] – [11], aspects have been dealt with, however, with the main emphasis on the latter. The various analyses have previously been presented at conferences (and thus published as conference papers) or in journals. The present report is mainly a collection of these papers. Further, a

paper describing a theoretical model for prediction of extreme shear will be presented at the special topic conference "The Science of making Torque form Wind" in Delft 19-21 April 2004 (Larsen, G.C. and Hansen, K.S.: "Statistical Model of Extreme Shear"). The latter paper is not included in the present report, although the work is partly related to the continuation of Annex XVII.

3 Fatigue loading

Concerning fatigue loading, two topics have been dealt with:

- Design turbulence intensity; and
- Spatial coherence.

The above listed topics are treated in two contributions. In the first contribution, a rational method for estimating design turbulence intensity as function of the wind speed has been demonstrated on turbulence measurements recorded at 6 different locations. Taking into account the variability of the turbulence intensity (here being described by a Log-Normal distribution), the design turbulence intensity has been estimated as function of wind speed for a moderately conservative Wöhler curve exponent (m=12).

The second contribution aims at calibrating the coherence description as given in the IEC 61400-1 standard. A substantial amount of full-scale wind field data, extracted from "Database on Wind Characteristics" (http://www.winddata.com/), has been analysed. The analysis was restricted to spatial coherence of the longitudinal turbulence component with special emphasis on vertical separation. Terrain- and atmospheric stability classifications have been merged into a classification according to the turbulence integral length scale. The measured coherences are thus parameterised in terms of turbulence integral length scale, measuring heights, (vertical/horizontal) spatial spacing and reduced frequency. A revised expression for the spatial coherence, associated with vertical separation, is presented and subsequently compared with measured coherences as well as with state-of-the-art coherence model predictions.

3.1 Design turbulence intensity

Kurt S. Hansen[1] and Gunner Chr. Larsen[2]

[1] Department of Mechanical Engineering, Fluid Mechanics, Nils Koppels Allé, DTU-Building 403,
Technical University of Denmark, DK-2800 Lyngby;
E-mail: ksh@mek.dtu.dk, Phone: +45 4525 4318, Fax: +45 4593 0663
[2] Risø National Laboratories, Wind Energy Department, P.O.48, DK-4000 Roskilde;
E-mail: gunner.larsen@risoe.dk, Phone: +45 4677 5056, Fax: +45 4677 5083

ABSTRACT: In order to continue cost-optimization of modern large wind turbines it is important continuously to increase the knowledge on wind field parameters relevant to design loads. This paper contains a parameterisation of the turbulence intensity at given sites, relevant for fatigue loading of wind turbines. The parameterisation is based on wind speed measurements extracted from the "Database on Wind Characteristics" (www.winddata.com). The parameterisation has been based on the Log-Normal distribution, which has proven to be a suitable distribution to describe the turbulence intensity distribution.

Keywords: Turbulence statistics, Log-Normal distribution,
wind simulation, wind turbines and fatigue.

1 INTRODUCTION

Wind turbine fatigue load cases as calculated according to the IEC 61400-1 standard. The design wind climate may be classified into a limited number of wind categories reflecting differences in terrains and of particular importance is the turbulence intensity as function of the wind speed. This is due to the close relationship between fatigue damage on a wind turbine and the wind field turbulence characteristics. Wind turbine operation is simulated using a synthetic wind time series with constant turbulence intensity representing each wind speed bin. According to previous analysis[2] the distribution of turbulence intensity can be assumed to follow a Log-Normal distribution.

This analysis contains a parameterization of the (Log-Normal) distributions according to terrain type and level. The analysis is based on a huge amount of wind field time series measured at different locations, which have been extracted from the "Database on Wind Characteristics"[3]. All time series were sampled with a frequency of 1 Hz or more, and all turbulence statistics represents a period of 10 minutes.

Finally, the quantiles in the estimated turbulence intensity distributions, corresponding to the specified design turbulence intensities in the IEC 61400-1 standard, are determined and assessed by means of a simple heuristic load model.

2 METHOD

The basic quantity used in this analysis is the measured turbulence intensity ti_{10} given by

$$ti_{10} = 100 \times \frac{\sigma_{10}}{V_{10}}, \tag{1}$$

where σ_{10} is the standard deviation of the wind speed and V_{10} is the mean wind speed, both with reference to the same 10 minute period.

2.1 Signal de-trending

ti_{10} may include a (trend) contribution from the mean level shift between two succeeding periods and this trend, which can be of a significant size is removed before the analysis can take place. The trend is assumed to be linear during the measuring period T (=600 s) according to:

$$V_{10} = k \times t + offset \tag{2}$$

The slope k is fitted with a least square method and the de-trended turbulence intensity ti_k is defined in :

$$V_k = V_{10} - (k/2) \tag{3}$$

$$ti_k = 100 \times \frac{\sqrt{\sigma_{10}^2 + k^2/12}}{V_k} \tag{4}$$

Eq. (3) indicates that the mean wind speed also is de-trended. Subsection 2.3 of this paper demonstrates the importance of this de-trending.

2.2 Log-Normal distribution

The definition and implementation of the LogNormal distribution are given[2] and this paper only resumes the definition in:

$$F(x, a_1, a_2) = \Phi\left(\frac{\ln(x) - a_1}{a_2}\right), \tag{5}$$

where Φ is the normal distribution. The Log-Normal distribution is defined according to the parameters (a_1,a_2). The mean value μ_k and the standard deviation σ_k of the distribution is expressed in terms of the parameters a_1, a_2 as

$$\mu_k = \exp(a_1 + a_2^2/2) \tag{6}$$

$$\sigma_k = \mu_k \times \sqrt{\exp(a_2^2) - 1} \tag{7}$$

2.3 Normal Score method

The implementation of the Normal Score plot method is described in[4] and the estimation of the Turbulence intensity Log-Normal distribution parameters are based on de-trended turbulence intensity values ti_k representing a wind speed bin of the size 1 m/s, where each observation represents a period of 600 seconds. The regression factor for the estimate of a_1 and a_2 is higher than 0.99, when using large populations.

2.4 Example

The procedure for the analysis is shown on Figure 1, and an example based on 1690 de-trended turbulence intensity observations, recorded 101m above ground level at Skipheia (N) has been demonstrated on Figure 2. The extracted, de-trended turbulence intensity values represent the wind speed interval from 15 to 16 m/s.

- Figure 1a) shows that the ranked observations (cdf vs. ln(ti_k)) exhibit an approximate linear relationship, indicating the underlying distribution being close to a Log-Normal distribution. The estimated regression values are: y=3.3765x-5.846; R^2=0.9927.
- Figure 1b) demonstrates the good agreement between measured and fitted distribution[1]. The figure includes the recommended IEC_B, class B turbulence intensity (15.6%), for the wind speed V=15.5 m/s, which corresponds to the 0.999 quantile. Furthermore the estimated design turbulence (9.6%; quantile=0.963), calculated according to (8) has been included

The estimated Log-Normal parameters (a1,a2) are listed in Table 1, both for the "trended" and de-trended time series.

Table 1: Example of de-trended signals

V=15±0.5 m/s	a1	a2	μ_k	σ_k
Raw signal	1.84	0.322	6.66	4.10
De-trended signal	1.73	0.296	5.90	3.46

The signal de-trending reduces the mean turbulence intensity level considerably (11%) at this site, but please note that the chosen example reflects the Atlantic weather system, which dominates by frequent front passages.

3 DATA MATERIAL

All the statistics, which are used for the analysis, are extracted form the Internet wind database "Database of Wind Characteristics"[3]. The sites have been selected to present different types of terrain (e.g. pastoral, coastal, complex and off-shore) and sites with long periods of wind field measurements (more than one year and more than 3 different levels).

Wind field measurements from the following sites have been included in the analysis:

Table 2: Measurement sites.

Site	Terrain	Height	Number of signals
Cabauw (NL)	Pastoral	200 m	5
Nasudden (S)	Coastal	118 m	5
Skipheia (N)	Coastal	101 m	4
Oak Creek (US)	Complex	79 m	4
Lysekil (S)	Complex	65 m	6
Horns Rev[2] (DK)	Off-shore	62 m	4

Only measurements from sectors with an uniform roughness has been included, and at coastal sites only measurements from "sea" direction has been included in the analysis.

[1] In order to obtain a high regression factor, a limited number (2-5%) of the observations in either the "high" and the "low" end of the ranked populations can be dropped without any significant influence due to the robustness of the method when using a large amount of observations.

[2] While no time series are available, de-trending has been impossible. The weather system at this site corresponds slightly to Skipheia (North Sea/ North Atlantic Sea) and the mean turbulence intensity should be reduced by 5 - 10% .

4 ANALYSIS

Initially all available time series, represented in Table 2 have been processed and the purpose is to categorize the turbulence intensity in terms of the parameters a_1, a_2 - as function of the wind speed. An indication of the measuring height has been included on all figures.

4.1 Categorisation of turbulence intensity

All the estimated parameters (a_1,a_2) are plotted as function of wind speed for each site on Figure 2a) and 2b) where each curve represents one level. Parameter a_1 decreases with height, while a_2 increases with height.

a) Figure 3a), site = Cabauw is based on a limited number of observation (600 hours). The parameter a_1 increases with the wind speed for heights larger than 20 m, while the parameter a_2 decreases for increasing wind speed. The parameter a_1 depends strongly of the height above ground level, while a_2 values converges for increasing wind speed.

b) Figure 3b), site = Nasudden is based on 2000 hours of measurements from a large sector with low, changing roughness. The parameter a_1 increases for increasing wind speed and depends of the height, while the parameter a_2 decreases but with a speed "lack" compared to the previous site.

c) Figure 3c), site = Skipheia is based on 6000 hours of measurements, primarily from an off-shore direction. The parameter a_1 increases with the wind speed, while the parameter a_2 decreases. This site demonstrates a clear behaviour of the turbulence intensity mainly due to the constant roughness.

d) Figure 4a), site = Oak Creek is based on 2000 hours of measurements in complex terrain. The parameter a_1 decreases with increasing wind speed, opposite to the previous results, while the parameter a_2 is more or less constant.

e) Figure 4b), site = Lysekil represent app. 12.000 hours of measurements from a limited complex terrain sector in the Swedish archipelago. The parameter a_1, decreases slightly with increasing wind speed while the parameter a_2 decreases. The plot reflects the large number of observations.

f) Figure 4c), site = Horns Rev is based on 12.000 hours of "trended" measurements. The turbulence parameter behaviour corresponds very much to Skipheia and the plot reflects the large number of observations.

The on-shore turbulence intensity is characterized with an increased parameter a_1 - as function of the wind speed while the offshore increases. The parameter a_2 for offshore sites decreases, while on-shore values shows more scatter. Both parameters depend strongly on height and roughness.

4.2 Distributions

Figure 5 shows the turbulence intensity distributions representing 4 different mean wind speeds (5.5,10.5,15.5 and 20.5 m/s) and at 4 different heights (58, 78, 98 & 118 m above ground level) reflecting the parameterisation given in Figure 3a. Figure 5 presents distributions for a representative coastal site and Figure 6 presents a complex site. Furthermore, Figure 5 and 6 include an indication of the recommended IEC turbulence intensity levels for all cases. The figures demonstrate the difference in the turbulence

intensity distributions between high and low wind speeds and between coastal and complex terrain. Furthermore the figures demonstrate the difference between the measured distributions and the recommended "constant" turbulence intensity value.

4.3 Design turbulence intensity

A representative design turbulence intensity can be calculated using formula (8), which has been adopted[2]. This formula assumes that the fatigue loading is purely generated from the stochastic part of the wind field leaving out the deterministic part and the selected Wöhler curve exponent of m=12 is conservative.

$$\sigma_{d,10}(U_{10}) = \left[\int_0^\infty P_\sigma\left(\sigma_{U,10} \mid U_{10}\right) \sigma_{U,10}^m \times d\sigma_{u,10} \right]^{1/m} \tag{8}$$

Only design turbulence for a representative wind turbine hub height (60 – 80m) have been analysed. Figure 7a) to 7f) shows the average and the design turbulence intensity corresponding to a Wöhler curve exponent m=12 for the sites. The IEC recommended turbulence levels has been included. Figure 7 shows that the design turbulence intensity partly agrees with the IEC recommended values (Cabauw, Nasudden, Oak Creek and Lysekil), while offshore-dominated climates seems to generate a smaller design turbulence, which agrees well with previous analysis[2].

The corresponding (conservative) quantile levels based on the estimated turbulence intensity distribution, with reference to the design turbulence and the recommended IEC turbulence level have been calculated as function wind speed and are shown on Figure 8a) to 8f).

The resulting quantile for the IEC turbulence increases is close to 1.0 for all wind speeds, while the design turbulence quantile decreases towards 0.8 for wind speeds above 15 m/s, except for the complex site.

5 CONCLUSION

A method for estimating design turbulence intensity as function of the wind speed has been demonstrated on turbulence measurements recorded at 6 different locations.
The analysis has demonstrated that signal de-trending reduces the mean turbulence intensity up to 11 % depending of site characteristics.

The design turbulence intensity as function of wind speed has been estimated for a number of future potential wind farm locations.

The quantile of the design turbulence intensity of to the IEC standard in work has been identified and seems to be higher than 80% for a conservative Wöhler curve exponent m=12.
The IEC recommended turbulence intensity corresponds to the conservative design turbulence intensity at wind speed below 15 m/s, while IEC values seems to be more conservative for wind speeds above 15 m/s except at complex sites.

6 RECOMMENDATIONS

To obtain suitable distributions of the turbulence intensity it is necessary to measure turbulence during 1 year as a minimum, depending on sectional roughness length.
Signal de-trending has to be included, while the trend contributions to the turbulence are not negligible and the trend is very site dependent.

7 REFERENCES

[1] IEC 61400-1, Wind turbine generator systems- Part 1: Safety requirements.
[2] Larsen, G.C, Off-shore fatigue turbulence (2001), Wind Energy, Vol.4, Issue 3, 2001.
[3] Database on Wind Characteristics, URL=http://www.winddata.com/.
[4] Gumbel, E.J., Statistics of Extremes (1966). Columbia University Express.

8 ACKNOWLEDGEMENTS

This analysis has benefited from measurements downloaded from the Internet database: "Database of Wind Characteristics" located at DTU, Denmark ("http://www.winddata.com/"). Wind field time series from the following sites have been applied: Cabauw (Royal Netherlands Meteorological Institute, KNMI), Näsudden (Dept. of Meteorology, Uppsala University), Oak Creek (Risø National Laboratories, Denmark) and Skipheia (Norwegian University of Science and Technology, Norway).

"Database on Wind Characteristics" was originally funded by EU – presently, the operation, development and maintenance are funded by IEA R&D Wind, Annex XVII.

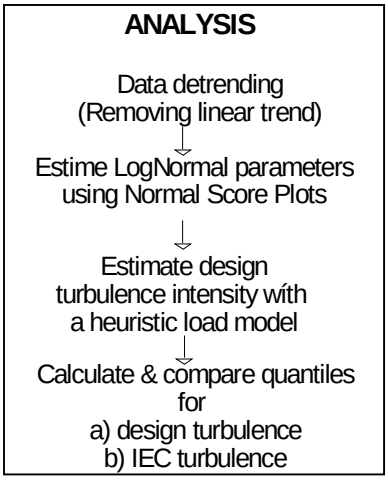

Figure 1: Flow chart for analysis of turbulence intensity measurements.

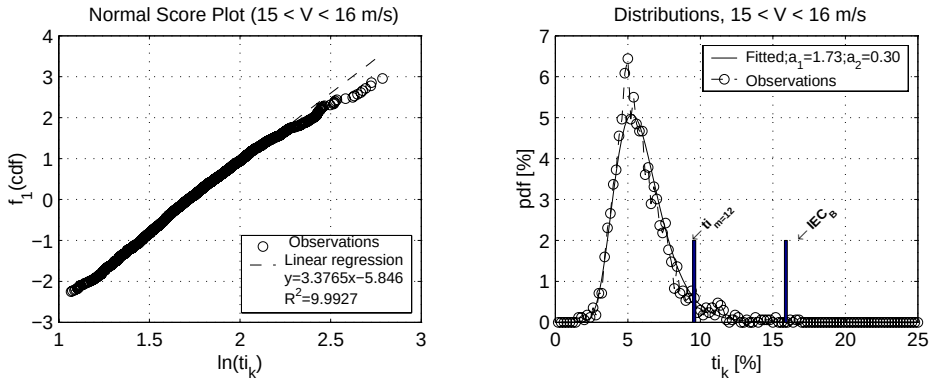

Figure 2: Example on how to determine the LogNormal parameters (a_1,a_2) and the resulting turbulence intensity distribution, based on measurements from Skipheia (N), level 101 m, 15 V < 16 m/s.

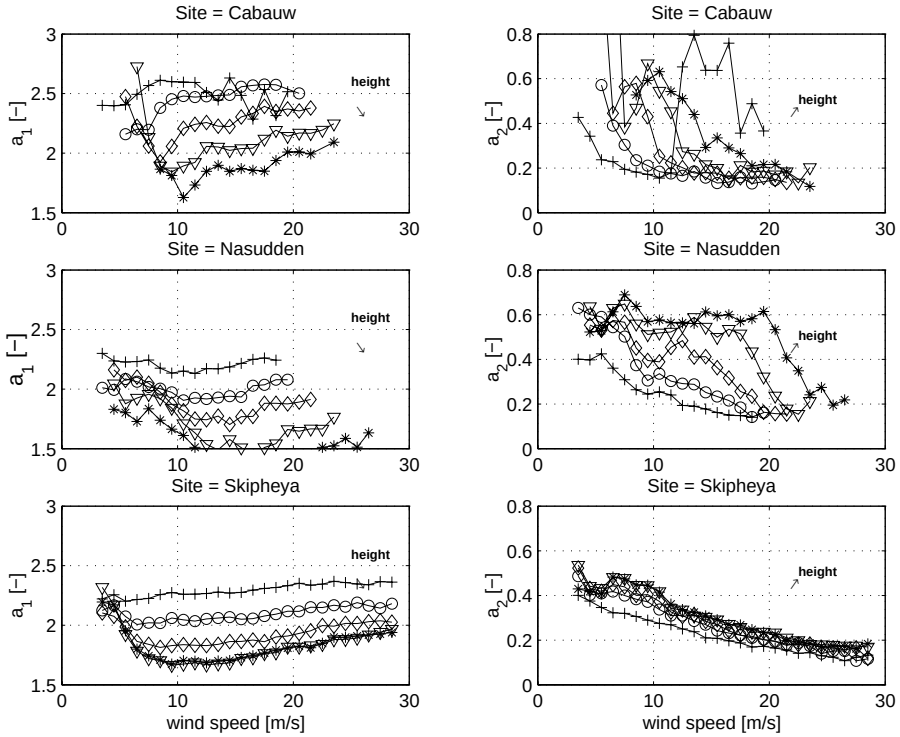

Figure 3: Estimated LogNormal parameters for site = Cabauw, Nasudden and Skipheia.

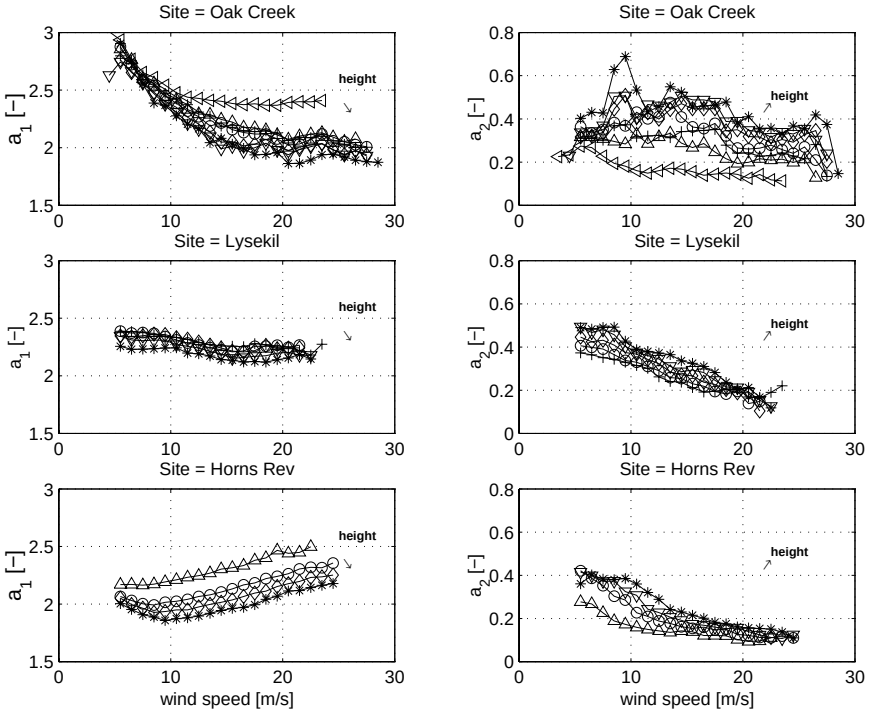

Figure 4: Estimated LogNormal parameters for site =Oak Creek, Lysekil and Horns Rev.

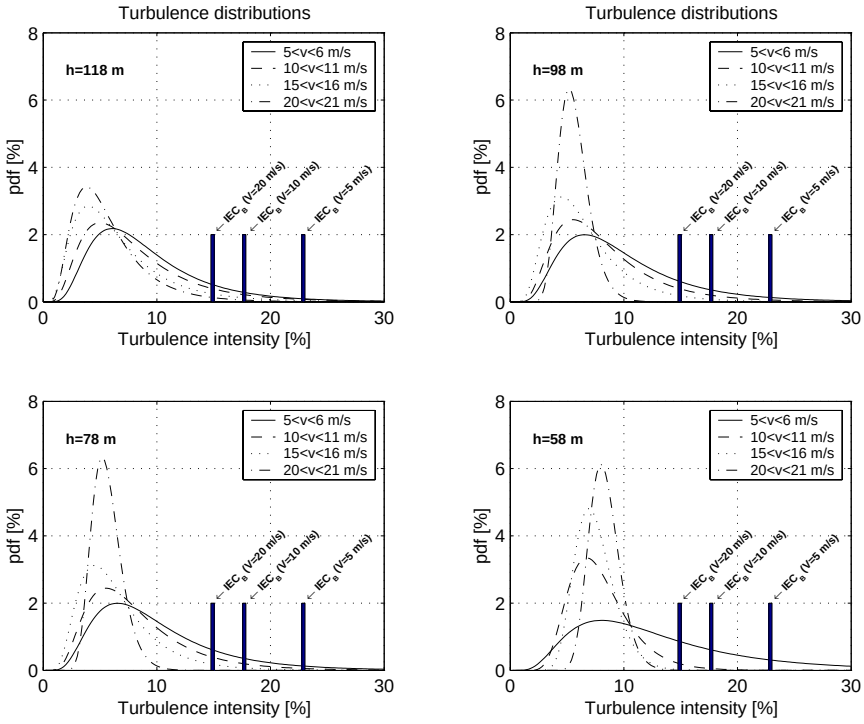

Figure 5: Estimated turbulence intensity distributions, site =Nasudden, h=58, 78, 98 & 118 m.

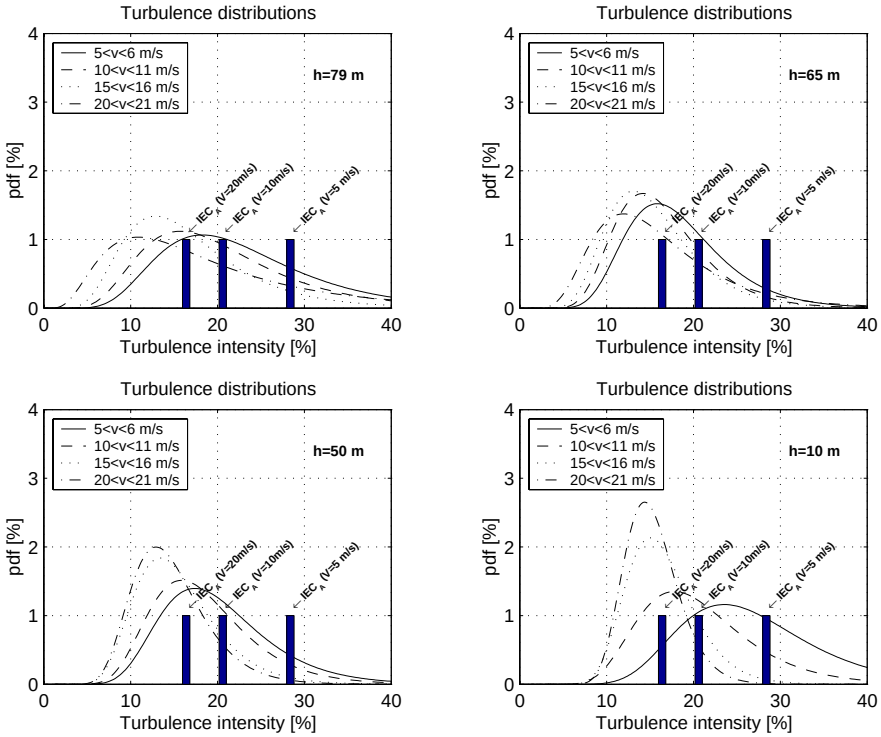

Figure 6: Estimated turbulence intensity distributions, site =Oak Creek, h=10, 50, 65 & 79 m.

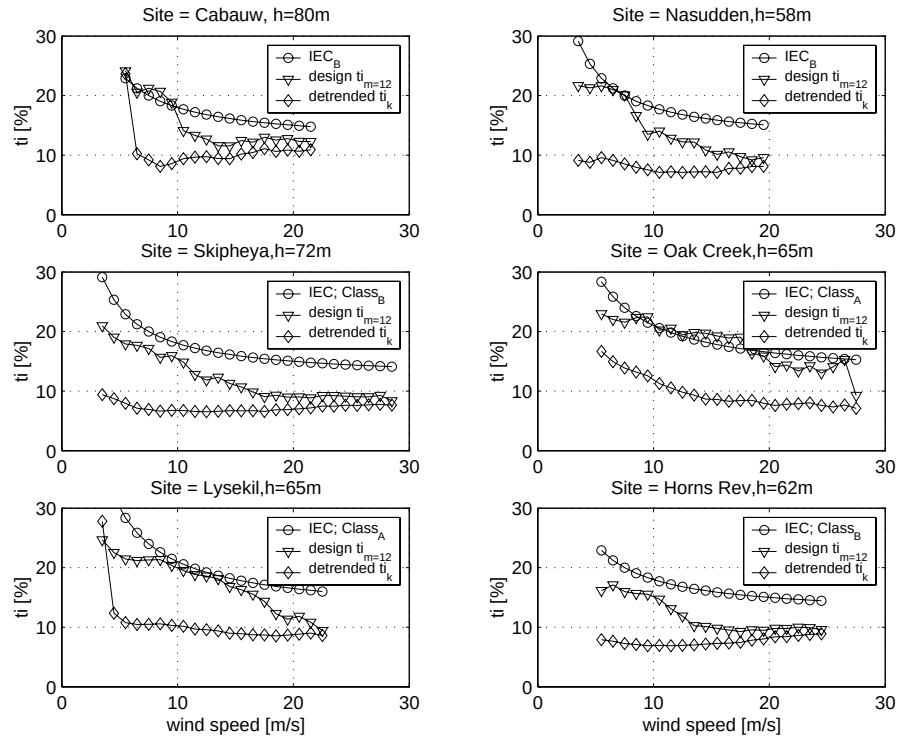

Figure 7: Estimated (conservative) design turbulence intensity, for 6 different sites, h = 60 – 80m.

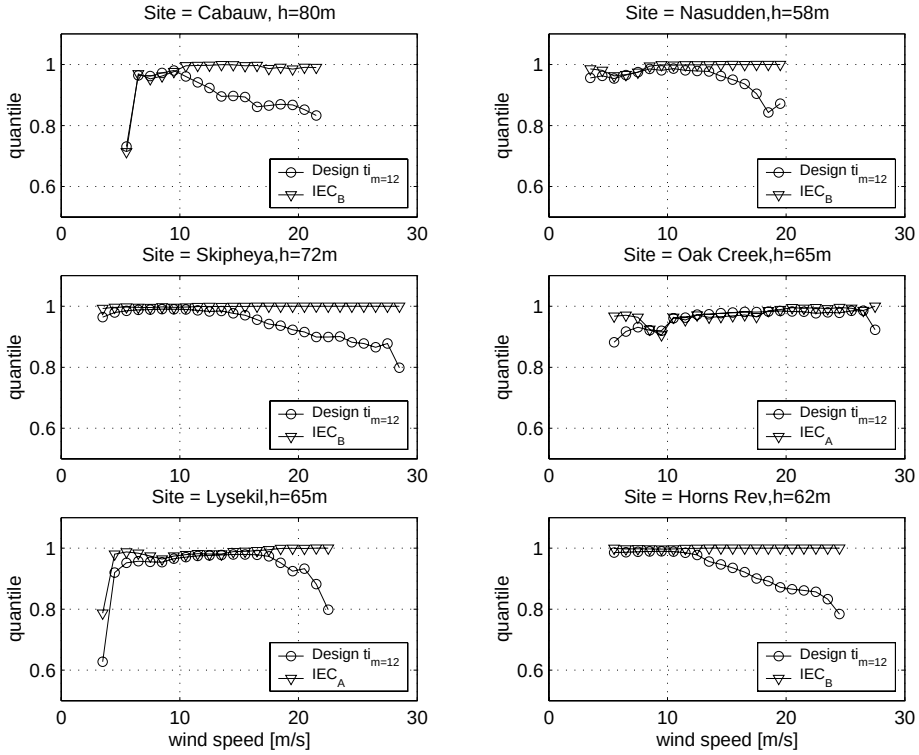

Figure 8: Estimated quantile levels for 6 different sites, h = 60 – 80 m.

3.2 Spatial coherence of the longitudinal turbulence

Gunner Chr. Larsen[1] and Kurt S. Hansen[2]
[1] Risø National Laboratories, Wind Energy Department, P.O. Box 49, DK-4000 Roskilde; E-mail: gunner.larsen@risoe.dk
[2] Department of Mechanical Engineering, Technical University of Denmark, DK-2800 Lyngby; E-mail:ksh@mek.dtu.dk

ABSTRACT: The design fatigue loading of wind turbine structures is traditionally determined from aeroelastic simulations, where a structural dynamic model is exposed to suitable synthetic turbulence wind fields. The wind fields are usually generated according to the recommendations given in the IEC 61400-1 standard, in which the turbulence is described combining the Kaimal spectrum with an exponential coherence model or, alternatively, by the Mann uniform shear spectral tensor. Recent investigations have shown that significant differences in simulated wind turbine tower fatigue loading may occur using the two suggested turbulence models. The differences in load predictions have been identified mainly to differences in the descriptions of the spatial coherence in the two turbulence models.
In order to calibrate the coherence descriptions given in the IEC 61400-1 standard, a substantial amount of full scale wind field data, extracted from "Database on Wind Characteristics" (http://www.winddata.com/), have been analysed. The analysis is restricted to spatial coherence of the longitudinal turbulence component, but both vertical and horizontal spatial separations have been investigated. Terrain- and atmospheric stability classifications have been merged into a classification according to the turbulence integral length scale. The measured coherences are thus parameterised in terms of turbulence integral length scale, measuring heights, (vertical/horizontal) spatial spacing, frequency and reduced frequency. Finally, a revised expression for the spatial coherence, associated with vertical separation, is compared with the measured coherences as well as with coherence predictions from the IEC 61400-1 standard as well as from the Mann model, and recommendations arising from this comparison are given.

Keywords: Coherence Models, Design Code, Turbulence, Turbulence Statistics, Spatial Coherence, Wind Field.

1 INTRODUCTION

Verification of the structural integrity of a wind turbine, according to the Draft IEC 61400-1 code [3], involves analysis of a number of fatigue load cases. The fatigue response is traditionally established using aeroelastic simulations, in which a dynamic model of the wind turbine is exposed to synthetic turbulence time series. The synthetic wind speed time series are usually generated based on knowledge to three basic turbulence characteristics - turbulence intensity, turbulence length scale and coherence.

The recommendations given in the IEC 61400-1 standard allow for two different turbulence descriptions. However, recent investigations [5] have shown that significant differences in simulated wind turbine tower fatigue loading may occur using the two suggested turbulence models. The differences in load predictions have been identified mainly to differences in the descriptions of the spatial coherence in the turbulence models.

For different terrain types, measuring levels and vertical spatial separations, the paper presents a calibration the coherence descriptions given in the existing IEC 61400-1 code for the longitudinal turbulence component.

2 THEORY

The coherence expresses the degree of agreement/correlation between (turbulence) structures, associated with two different (stationary) time series, disregarding possible phase shifts between such structures. Mathematically, the coherence is defined as normalised squared cross-spectrum amplitudes, with the normalising factors being the product of their two respective auto-spectrum amplitudes. As both the cross-spectra and the auto-spectra depend on the frequency, the coherence will also depend on the frequency, simply meaning that the agreement between (turbulence) structures depends on their scale. The coherence takes (real) values between zero and one.

Let us consider two (turbulence) wind speed time series $u_1(t)$ and $u_2(t)$ with Fourier transforms $U_1(\omega)$ and $U_2(\omega)$, respectively. Thus

$$U_i(\omega) = F[u_i(t)] \; ; \; i = 1,2 \,, \tag{1}$$

where F[∗] denotes the Fourier operator. The spectrum expresses the distribution of the energy contained in the turbulence structures on different scales. Following the definition of (one sided) spectra in [2], for sample records of length T, the auto- and cross-spectra related to the stochastic signals $u_1(t)$ and $u_2(t)$ are given by

$$S_i(\omega) = \lim_{T\to\infty} \frac{2}{T} \left\langle U_i(\omega) \overline{U_i}(\omega) \right\rangle \; ; \; i = 1,2 \,, \tag{2}$$

and

$$S_{12}(\omega) = \overline{S_{21}}(\omega) = \lim_{T\to\infty} \frac{2}{T} \left\langle U_1(\omega) \overline{U_2}(\omega) \right\rangle \,, \tag{3}$$

respectively, where ⟨∗⟩ denotes an ensemble averaging operator. Note, from equations (2) and (3) that the auto-spectra are real quantities, whereas the cross-spectra generally are complex.

The coherence is now expressed as

$$\gamma_{12}(\omega) = \gamma_{21}(\omega) = \frac{S_{12}(\omega)\overline{S_{12}}(\omega)}{S_1(\omega)S_2(\omega)} = \frac{S_{21}(\omega)\overline{S_{21}}(\omega)}{S_2(\omega)S_1(\omega)} \,, \tag{4}$$

from which it is easily seen that the coherence depends on frequency and further is a real quantity (between 0 and 1), reflecting that phase shifts have been disregarded. The coherence, as given by expression (4), refer to spectra determined from ensemble averaging. This is, however, an theoretical abstraction, and in practice the ensemble averaging is replaced by averaging of spectra corresponding to a finite number of consecutive time samples (of equal length). The cost is that a bias is introduced in the coherence estimate. For an averaging with N statistical degrees of freedom (i.e. based on N independent time series) the *mean* estimated coherence, $E[\gamma_{12,est}(\omega)]$, relates to the true coherence as [6]

$$E[\gamma_{12,est}(\omega)] = \gamma_{12}(\omega) + \frac{(1-\gamma_{12}(\omega))^2}{N} \,, \tag{5}$$

from which the true coherence is easily determined from

$$\gamma_{12}(\omega) = \frac{2 - N + \sqrt{(N-2)^2 - 4(1 - NE[\gamma_{12,est}(\omega)])}}{2}, \tag{6}$$

which especially for coherences close to zero can (depending on the magnitude of N) result in a significant correction. Note, that in case the number of averaged elements is one (i.e. no averaging) the coherence is identical one, which can easily be verified by combining equations (3), (4) and (5).

The agreement between turbulence structures, inherent in two time series, will, apart from the frequency, also depend on the *relative* spatial position of the associated two measuring points, presuming that the turbulence field can be considered homogeneous. For inhomogeneous turbulence fields the dependence is on the *absolute* spatial position of the measuring points.

In the atmospheric boundary layer the observed spectra depend on the particular site conditions (including the thermal conditions) and the measuring height. One way to categorise *measuring site* is therefore through the integral length scale which both quantify the turbulence spectral dependence on site and thermals. The *inhomogeneous character* of turbulence in the atmospheric boundary layer is taken into account in the analysis by categorising the available measurements according to their measuring height above terrain *and* according to whether the measuring points are displaced vertically or horizontally.

In summary, the investigated coherences are categorised according to:

- Mean of the integral length scale associated with the two investigated turbulence time series;
- Mean of the involved measuring heights above terrain;
- Spatial displacement of the associated two measurement points; and
- Whether the measurement points are displaced vertically or horizontally.

Except for the integral length scale all the parameters defining the applied data material categories are immediately available from "Database on Wind Characteristics" [4]. The integral time scale, L^T_i, associated with the turbulence time series $u_i(t)$ is in the analysis defined as

$$L_i^T = \frac{1}{\xi^2}\int_0^T S_i\left(\frac{1}{\tau}\right)\tau\, d\tau \;;\; i=1,2 \;, \tag{7}$$

with

$$\xi_i^2 = \int_0^T S_i\left(\frac{1}{\tau}\right) d\tau \;;\; i=1,2 \;. \tag{8}$$

The integral length scale, L^L_i, is simple derived from the integral time scale by multiplication with the mean wind speed, $\bar{u}_i$, again assuming stationary processes. Thus

$$L_i^L = \bar{u}_i L_i^T \;;\; i=1,2 \;. \tag{9}$$

At a first glance, the cogent mathematical definition of the turbulence length scale as given above has the drawback that it in particular depends on the properties of the spectrum at low frequencies where the statistical significance of the spectral estimates are limited. This fact is, however, also reflected in the estimation of the coherence, where significant coherences are related to low frequencies and thereby also subjected to limited statistical significance. Thus, in this respect the present length scale definition and the coherence estimates are "consistent".

Empirical investigations show that the *coherence decay*, which is the essential/core topic for the present investigation, usually is associated with *reduced frequencies* below of

the order 0.5. The reduced frequency, f_r, is defined as

$$f_r = \frac{fD}{\overline{u}}, \tag{10}$$

where f is the frequency (in Hz) and D is the spatial displacement associated with the coherence parameter. The reduced frequency expresses the proportion between the spatial separation and a characteristic turbulence eddy size related to the frequency f.

The coherence is intimately related to the auto- and cross-spectral properties, and from the above discussion it is therefore obvious that the coherence decay is primary related to the spectral properties in the frequency regime [0; f_r]. As a consequence it is felt that, for the present purpose, the integral length scale given by equations (8), (7) and (6) is well suited as a representative (single) scale parameter for the spectral regime controlling the coherence decay.

3 DATA MATERIAL

The coherence, as described in Section 2, has been analysed based on a large number of full-scale wind speed measurements extracted from "Database on Wind Characteristics" [4]. Only the horizontal turbulence component has been investigated, meaning that both cup anemometer and sonic measurements apply. However, the present investigation is solely based on cup anemometer measurements.

The sites have been selected to represent different types of terrain (flat homogeneous, coastal terrain and off-shore conditions). In the selection of sites, care have further been taken to assure that for each site category

- A large data material is available, reflecting representation of a reasonable large mean wind speed range;
- (If possible) a suitable range of vertical spacings are available, reflecting relevant wind turbine sizes;
- (If possible) at least one horizontal spacing is available.

The resulting sites with their key characteristics are specified in Table 1.

Skipheia	Hill	Coastal	H/V	5-32m/s
Cabauw	Flat	Pastoral	V	5-26m/s
Ciba	Flat	Pastoral	V	5-15m/s
Alsvik	Flat	Coastal	H	5-20m/s
Näsudden	Flat	Coastal	V	5-24m/s
Middelgrund	Flat	Off-shore	V	5-16m/s
Gedser Rev	Flat	Off-shore	V	5-16m/s
Rodsand	Flat	Off-shore	V	5-19m/s

Table 1: Site characteristics. "V" and "H" denotes that vertical and horizontal spacings are available.

Some of the selected sites offer mean wind speed values below 5m/s, however, in the present analysis only coherences associated with mean wind speeds above 5m/s are considered.

The amount of analysed data varies somewhat between the sites (Skipheia: 3290 hours; Cabauw: 473 hours; Ciba: 282 hours; Alsvik: 1740 hours; Näsudden: 2292 hours; Middelgrund: 1224 hours; Gedser Rev: 563 hours and Rødsand: 587 hours).

4 APPROACH

The present analysis is restricted to coherence behaviour in undisturbed wind fields. Therefore, measurements associated with wind turbine wake situations and measurements affected by flow distortion caused by the meteorological mast etc. have initially been discharged.

The remaining data sets have subsequently been classified according to *site*, (mean) *measuring height*, *integral length scale* and *spatial displacement* of the involved two sensors.

Basically, two different classes of spacings are considered - *vertical* spacings and *horizontal* spacings. Within each of these classes, only spacing distances of certain sizes, compared to the (mean) measuring heights, are considered. The idea behind this restriction is that the spacing distance, for a given (mean) measuring height, must correspond to a characteristic dimension of a rotor, with a hub height corresponding to the (mean) measuring height, in order to reflect the important wind turbine loadings. The following range of spacing/height ratio has (rather arbitrary) been selected

$$0.5 \le \frac{D}{\overline{h}} \le 1.5 \ , \tag{11}$$

where $\overline{h}$ denotes the mean height of the relevant sensors. To address realistic wind turbine sizes, only mean measuring heights above 25*m* are considered.

The integral length scale classification reflects the turbulence characteristics of importance for the coherence behaviour (i.e. the terrain effect as well as the thermal impact on turbulence spectra condensed in only one descriptive parameter).

For a given "pair" of wind speed time series, belonging to an arbitrary bin class in the classification system, the data analysis is performed as follows:

- The two time series are chopped into a suitable number of segments (50% overlap have been selected) in order prepare for the spectral averaging specified in equations (2) and (3). The number of segments depends on the total length of the selected time series, and typically each segment represents a time span of the order of 5-10 minute.
- The DC component of the time segments are subtracted and the resulting time segments are detrended (linear trend assumed)
- For each segment "pair" the auto- and cross-spectra are evaluated using a FFT algorithm combined with a Hanning window, and, based on these, the average spectra are subsequently determined.
- The coherence is determined based on the averaged spectra in accordance with equation (4), and subsequently bias-corrected in accordance with equation (6). Finally, the integral length scales, associated with the two data segments, are determined based on the average spectra in accordance with equation (7) and (8), and the arithmetic mean of these are used as the length scale classification parameter for the computed coherence.

The coherence is tabulated as function of the reduced frequency defined by equation (9), and for each particular (site, height, spacing and integral length) bin class, the available coherence data are further collected in bins of the reduced frequency. The coherences belonging to each particular reduced frequency bin are finally averaged, giving the resulting coherence in terms of reduced frequency.

5 RESULTS AND DISCUSSION

The Skipheia site is outstanding both in respect to the extend of the available data material and in respect to the spatial resolution (vertical as well as horizontal) of the wind speed sensors. Therefore, the main emphasis has been put into the analysis of the data material from this site, and, as a logical consequence, the empirical coherence model to presented in Section 6 is also based on these results. The analysis of the data material from the remaining sites has primary been used to support conclusions resulting from the Skipheia analysis.

Both vertical and horizontal separation have been investigated, and in particular for the vertical separation a substantial data material is required because of an applied direction binning in the mean wind direction, which reduces the available data material substantially.

5.1 Vertical separation

For coherence analysis associated with vertical separations no direction binning is necessary, and the full data set is therefore available for the analysis. For the Skipheia site the following combinations of mean heights (h) and separations (D) have been analysed: D30h26, D31h56, D51h46, D60h71, D61h42 and D80h61. For the remaining sites, the height/separation specifications are in the same "regime" except for the Cabauw site which offers especially large mean heights and separations (D40h60, D60h50, D60h110, D100h90, D120h80, D120h140, D160h120).

Examples of measured coherences from the Skipheia site are shown in Figures 1, 2 and 3.

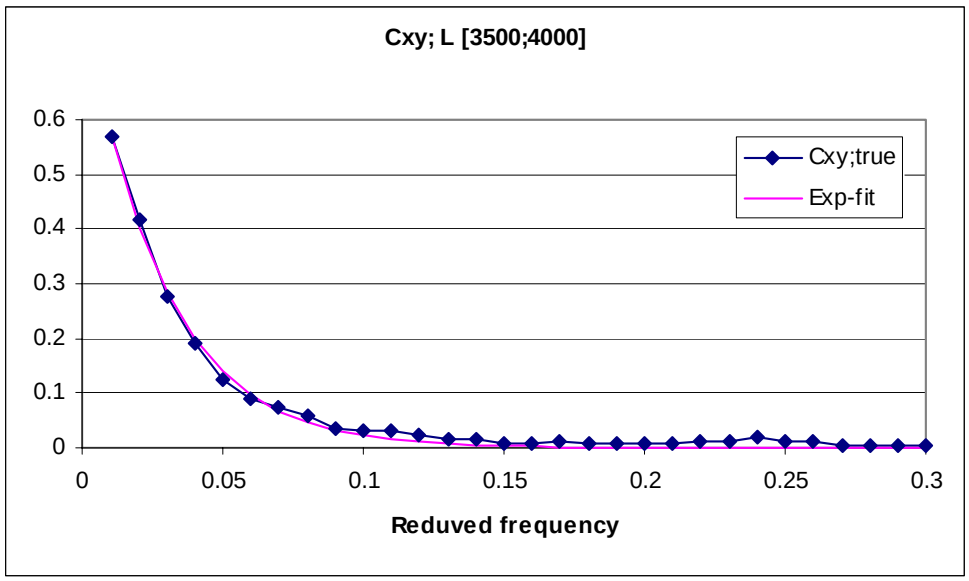

Figure 1: Coherence corresponding to a mean height equal to 26 m, a vertical spacing equal to 30 m and a length scale in the interval [3500;4000].

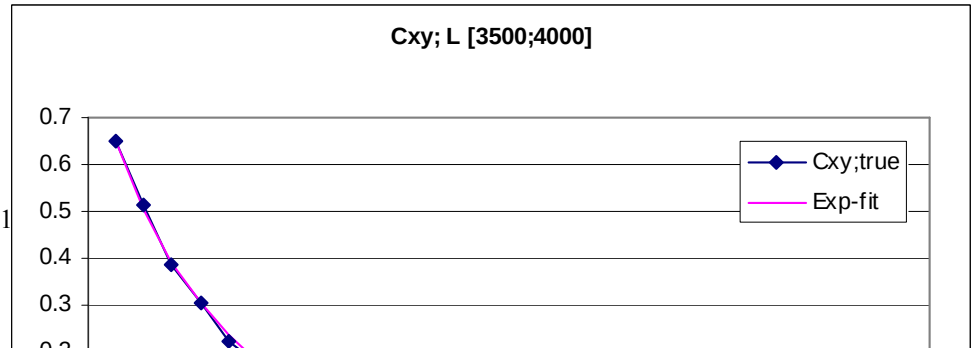

Figure 2: Coherence corresponding to a mean height equal to 56 m, a vertical spacing equal to 31 m and a length scale in the interval [3500;4000].

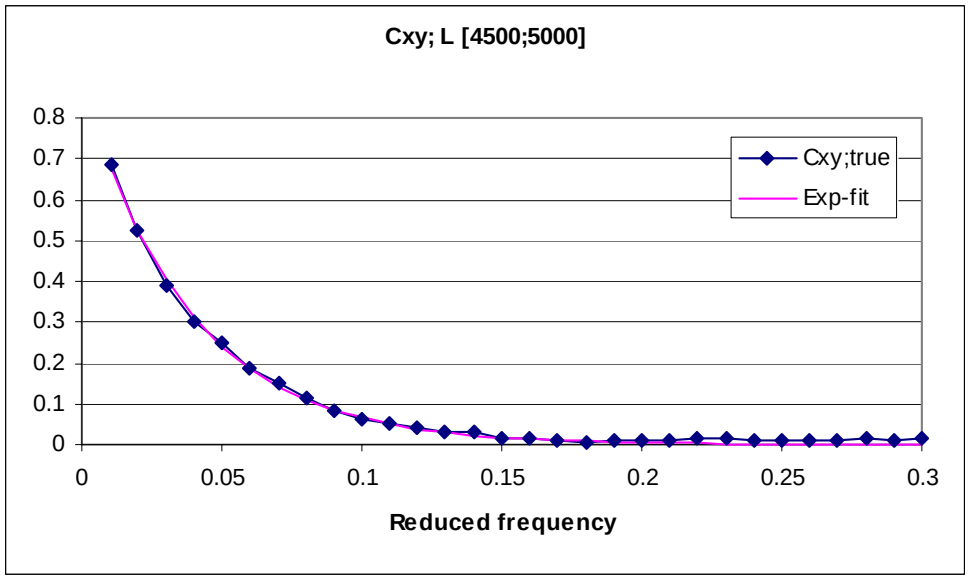

Figure 3: Coherence corresponding to a mean height equal to 56 m, a vertical spacing equal to 31 m and a length scale in the interval [4500;5000].

The following qualitative conclusions can be drawn based on the results from the analysed sites:

- The coherence increases with increasing mean height (which is also reflected comparing Figure 1 and Figure 2);
- The coherence decreases with increasing separation;
- The coherence increases with increasing length scale (which is also reflected comparing Figure 2 and Figure 3).

The above coherence dependencies have basically the same physical background.
The dependence of the coherence with height relates to the fact that not all (large) turbulence scales are represented "close" to the surface, and that an increasing portion of these large scales tend to be represented as the measuring height is increased.

The dependence of the coherence with separation reflects that large turbulence scales are less frequent represented that smaller turbulence scales, and that coherence for large separations are associated with large turbulence scales.

The dependence of the coherence with turbulence length scale relates physically to the fact that large turbulence scales are better represented in turbulence spectra with large length scales.

5.2 Horizontal separation

Two sites, Alsvik and Skipheia, provide possibilities for analysis of coherence associated with a horizontal separation. Unfortunately, only rather large separation distances are available (ranging between 79 m and 170 m).

Analysis of coherence associated with horizontal separation requires wind direction binning in order to assure that no (or only limited) turbulence "offset" between the relevant two sensors takes place. The direction binning is a compromise between data reduction and turbulence "offset". For the present analysis, a +/- 18 deg. sector was selected corresponding to a longitudinal "offset" of the turbulence of maximal 5% of the spatial separation.

For the Skipheia site the following combinations of mean heights and separations have been analysed: D79h21, D79h41, D79h101, D170h21 and D170h41. For the Alsvik site the corresponding height/separation combinations are: D112h24, D112h31, D112h36, D112h41 and D112h53.

An example of measured horizontal coherences from the Skipheia site is shown in Figure 4.

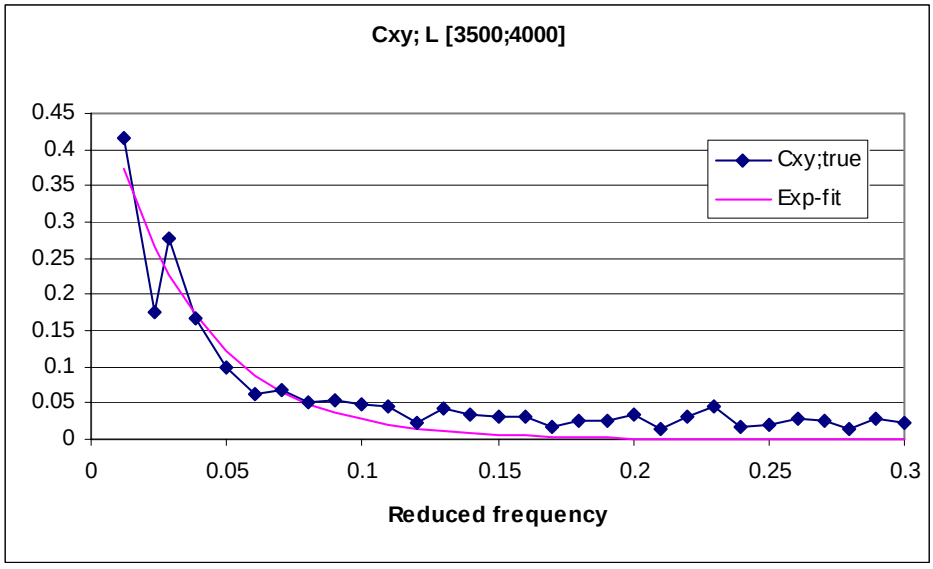

Figure 4: Coherence corresponding to a mean height equal to 41 m, a horizontal spacing equal to 79 m and a length scale in the interval [3500;4000].

As a result of the more limited data material, the coherences, corresponding to horizontal displacements, are less statistical significant than the coherences determined for the vertical displacements. The dependence of the coherence on spatial separation and length scale seems not consistent, whereas most of the measurements display increasing coherence with increasing altitude of the sensors.

6 EMPIRICAL MODEL

The comprehensive results from analysis of the vertical coherences from the Skipheia site has been used to derive an empirical model for the coherence as function of reduced

frequency, vertical separation, altitude and turbulence length scale (as defined in equation (9)).

Initially, tree different types of fits were applied on the coherence data emerging from the data analysis - a traditionally 2-parameter exp-fit, a 3-parameter exp-fit and a 2-parameter sech-fit. The investigation showed that the 3-parameter exp-fit performed marginally better than the 2-parameter exp-fit, which again performed marginally better than the 2-parameter sech-fit. Based on this observation, and a wish to limit the number of model parameters as mush as possible, it was decided to base the empirical model on an expression of the generic form

$$\gamma_{12}(f_r) = Exp\left[C_1(D,h,L^L) f_r + C_2(D,h,L^L)\right] , \tag{12}$$

where $C_1(D,h,L^L)$ is a *shape* parameter and $C_2(D,h,L^L)$ is a *scale* parameter. A priori it is known that both parameters must be negative in order that (12) comply with the basic features of a coherence function.

Based on the measured coherences, the shape and scale parameters are parameterised in two steps. First step relates to the turbulence length scale. Guided by the data material the following generic form of the length scale parameterisation is assumed

$$\begin{aligned} C_1(D,h,L^L) &= E_1(D,h)L^L + E_2(D,h) , \\ C_2(D,h,L^L) &= -Exp\left[F_1(D,h) - F_2(D,h)L^L\right] . \end{aligned} \tag{13}$$

Examples of the experimental results leading to the parameterisation (13) are given in Figures 5 and 6.

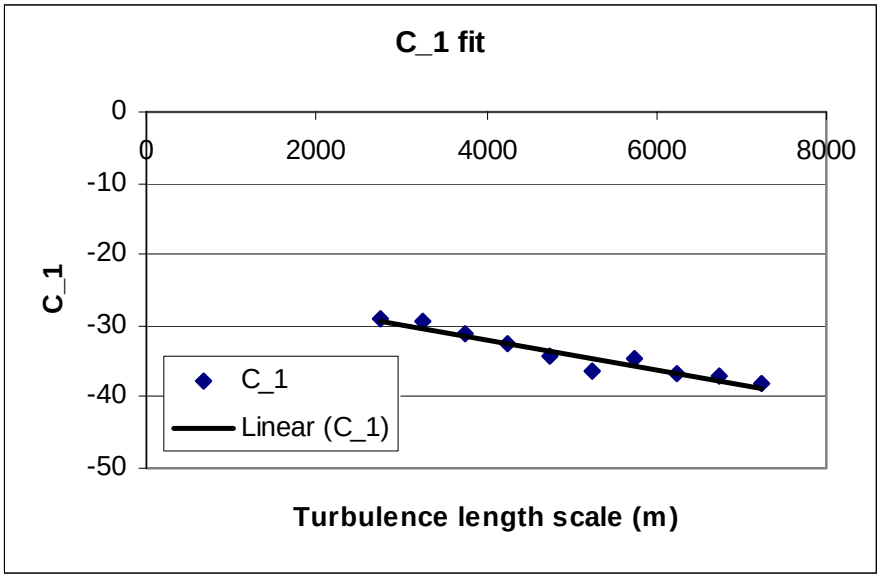

Figure 5: C_1-parameterisation resulting from Skipheia D51h46.

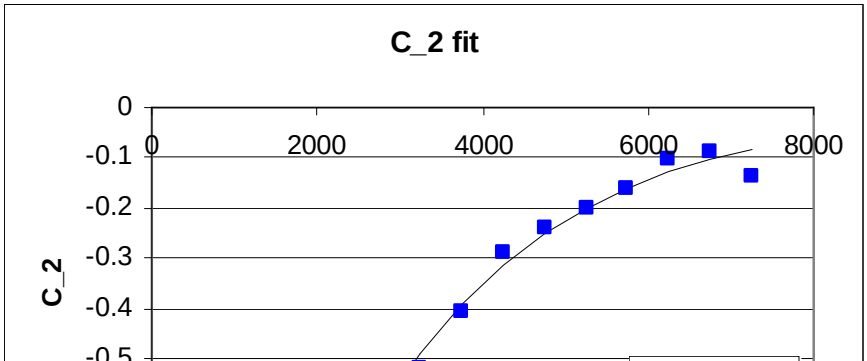

Figure 6: C_2-parameterisation resulting from Skipheia D51h46.

The second step of the parameterisation relates to the separation and altitude parameters. Assuming that the gradients $\delta E_1/\delta D$, $\delta E_1/\delta h$, $\delta E_2/\delta D$, $\delta E_2/\delta h$, $\delta F_1/\delta D$, $\delta F_1/\delta h$, $\delta F_2/\delta D$ and $\delta F_2/\delta h$ asymptotically approach zero for D and h (individually) approaching infinity, we (otherwise rather arbitrary) assume the following generic expressions for the $E_i(D,h)$ and the $F_i(D,h)$ functions (i = 1,2)

$$\begin{aligned} E_i(D,h) &= a_i D^{1/3} + b_i D^{1/3} h^{1/3} + c_c h^{1/3} + d_i + e_i D^{2/3} + f_i h^{2/3} , \\ F_i(D,h) &= \hat{a}_i D^{1/3} + \hat{b}_i D^{1/3} h^{1/3} + \hat{c}_c h^{1/3} + \hat{d}_i + \hat{e}_i D^{2/3} + \hat{f}_i h^{2/3} . \end{aligned} \tag{14}$$

The values of $E_i(D,h)$ and $F_i(D,h)$ is known in certain points (D,h) from the Skipheia results (i.e. (30,26), (31,56), (51,46), (60,71), (61,42) and (80,61)). In addition, the data material allows the gradients $\delta E_1/\delta D$, $\delta E_2/\delta D$, $\delta F_1/\delta D$ and $\delta F_2/\delta D$ to be determined for h approximately equal to 60 m (combining the D36h56 and the D80h61 results), and the gradients $\delta E_1/\delta h$, $\delta E_2/\delta h$, $\delta F_1/\delta h$ and $\delta F_2/\delta h$ to be evaluated for D approximately equal to 30 m (combining the D30h26 and the D31h56 results) and approximately equal to 60 m (combining the D61h42 and the D60h71 results).

The parameters in equation (14) are determined using a least square optimisation in which the available values of the $E_i(D,h)$ and $F_i(D,h)$ functions as well as their gradients are included. The reason for including the gradients (explicitly) is that we want to emphasise the observed coherence dependence on the altitude h and the spatial separation D. Thus the parameters in (14) are determined as the sets $(a_i, b_i, c_i, d_i, e_i, f_i)$ and $(\hat{a}_i, \hat{b}_i, \hat{c}_i, \hat{d}_i, \hat{e}_i, \hat{f}_i)$ that minimises the functionals

$$\begin{aligned} &\Pi(a_i, b_i, c_i, d_i, e_i, f_i) = \\ &\sum_{j=1}^{6}\left[E_i(D_j,h_j) - M\{E_i(D_j,h_j)\}\right]^2 + \sum_{j=7}^{8}\left[\frac{\partial E_i}{\partial h}(D_j,h_j) - M\left\{\frac{\partial E_i}{\partial h}(D_j,h_j)\right\}\right]^2 + \left[\frac{\partial E_i}{\partial D}(D_9,h_9) - M\left\{\frac{\partial E_i}{\partial D}(D_9,h_9)\right\}\right]^2 , \end{aligned} \tag{15}$$

and

$$\begin{aligned} &\Theta(a_i, b_i, c_i, d_i, e_i, f_i) = \\ &\sum_{j=1}^{6}\left[F_i(D_j,h_j) - M\{F_i(D_j,h_j)\}\right]^2 + \sum_{j=7}^{8}\left[\frac{\partial F_i}{\partial h}(D_j,h_j) - M\left\{\frac{\partial F_i}{\partial h}(D_j,h_j)\right\}\right]^2 + \left[\frac{\partial F_i}{\partial D}(D_9,h_9) - M\left\{\frac{\partial F_i}{\partial D}(D_9,h_9)\right\}\right]^2 , \end{aligned} \tag{16}$$

respectively, where (D_j,h_j), $j = 1, \ldots, 9$ denotes the parameter combinations in which values of either the functions $E_i(D,h)$ and $F_i(D,h)$ or their gradients have support in the analysed coherence data. M{*} is the measurement operator giving the measured value of the argument.

The derived empirical is finally constrained to ensure that the scale parameter $C_2(D,h,L^L)$ is monotone with respect to (h,L^L).

7 MODEL COMPARISONS

The empirical model developed (based on the Skipheia measurements) in previous section has been compared with measured coherences from *other* sites (Cabauw, Näsudden, Middelgrund, Gedser Rev and Rodsand) where it performs satisfactory, however, with a slight overestimation of the Näsudden results. The deviation between model and data in the case of Näsudden can be explained by the fact that the measured coherences for these two sites also differ, with the Skipheia coherences exceeding the Näsudden coherences.

The model has also been compared with predictions from other available models (the Mann-model [7] and the IEC-model [3]). Both the IEC-model and the Mann-model include a dependence on the turbulence length scale, however, for non of these models the length scale classification according to equation (9) has been performed. As the variation of the coherence with the length scale can be substantial, it was decided to base the comparison on data and empirical model predictions ranging from low length scales (L^L = 2750 m) to large length scales (L^L = 6750 m). The result is shown in Figure 7.

For the investigated data, the decay of the Mann coherence resembles the decay of the measured data as well as the empirical model, however with a tendency to slower decay. The decay of the IEC-model is much slower than for the measured coherences and the other two models.

The scale of the coherence depends significant on the turbulence length scale. The magnitude predicted by the IEC-model corresponds to the magnitude for measurements associated with low turbulence length scales. The magnitude predicted by the Mann-model corresponds to the measured coherences associated with large turbulence length scales.

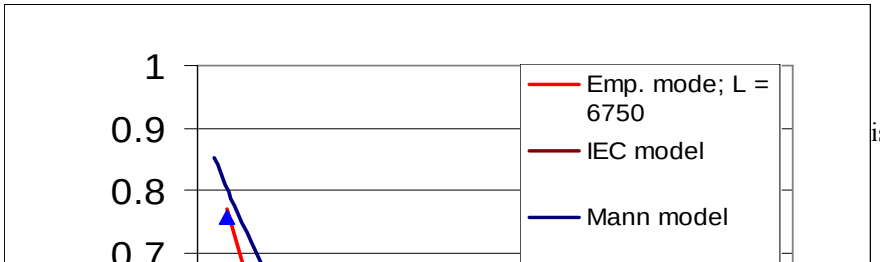

Figure 7: Comparison of coherence predictions and measured coherences (Skipheia; D = 31m, h = 56 m).

8 CONCLUSION

An extensive amount of high sampled (horizontal) wind speed measurements from different sites have been analysed with respect to coherence behaviour. Both coherences associated with vertical and horizontal spatial separations have been investigated. However, for the coherences related to horizontal spatial separations, the data material is not consistent with respect to the dependence of the coherence with turbulent length scale and spatial separation, whereas the measured coherences clearly indicate increases levels with increasing measuring altitude and decreasing levels with increasing (reduced) frequency.

For the coherences associated with vertical separations the following qualitative conclusions can be drawn:

- The coherence decay with increasing (reduced) frequency;
- The coherence decay with increasing spatial separation;
- The coherence increase with increasing turbulence length scale; and
- The coherence increase with increasing measuring altitude.

The measured coherences associated with vertical spatial separations have been used to develop and calibrate an empirical coherence model. The empirical model has been demonstrated to fit well with the available data, however, with a slight overestimation of the Näsudden results.

The empirical model have subsequently been compared with measured coherences arising from the analysis as well as with coherences predicted by the Mann-model and the IEC-model. Although some uncertainty exists about the turbulence length scale (in the equation (9) sense) used in the Mann and the IEC predictions, the Mann-model seems to resemble the measured data (and the predictions from new empirical model) better than the IEC-model.

ACKNOWLEDGEMENTS

The Danish Energy Agency funded the present work under the contract ENS 1363/02-0013.

Further, the analysis has benefited from measurements downloaded from the Internet database: "Database of Wind Characteristics" located at DTU, Denmark. Internet: "http://www.winddata.com/". Wind field time series from the following sites has been applied: Cabauw (Royal Netherlands Meteorological Institute, KNMI), Näsudden and Alsvik (Dept. of Meteorology, Uppsala University), Middelgrunden, Gedser Rev, Rødsand and Ciba (Risø National Laboratories, Denmark), and Skipheia (Norwegian University of Science and Technology, Norway).

Finally, our colleague Jacob Mann is acknowledged for providing coherences predicted by the Mann turbulence model.

9 REFERENCES

[1] Panofsky, H.A. and Dutton, J.A. (1984). Atmospheric Turbulence - Models and Methods for Engineering Applications. John Wiley & Sons.

[2] Bendat, J.S. and Piersol, A.G. (1995). Random Data - Analysis and Measurement Procedures. John Wiley & Sons.

[3] IEC 61400-1 Wind Turbine Safety System: part 1, Safety Requirements.

[4] Database on Wind Characteristics. http://www.winddata.com/.

[5] Thomsen, K. (2002). The Impact of Turbulence Modelling on Tower Loads (in Danish).Risø-I-1909.

[6] Koopmans, L.H. (1974). The Spectral Analysis of Time Series. Academic Press.

[7] Mann, J. (1994). The Spatial structure of Neutral Surface-layer Turbulence. Journal of Fluid Mechanics, v. 273, pp. 141-168.

4 Ultimate loading

As for the ultimate loading, the focus has been on

- Extreme wind speed gust loading; as well as on
- Extreme shear load conditions.

Three contributions concern extreme wind speed gust loading. In the first contribution, a general statistical method that, based on experimental observations, can be applied to estimate the probability density function for extreme wind speed events, corresponding to an arbitrary recurrence period, is presented. This method is subsequently applied on two data sets, representing offshore locations with different characteristics - coastal ocean waters as well as more constrained inner Danish waters. In the second contribution, a rational method to calibrate the Extreme Operating Gust (EOG) magnitudes, as specified in the IEC 61400-1 code, is presented. This method combines a wavelet expansion with extreme statistics and results in consistent estimates of wind speed gust magnitudes for arbitrary return period, mean wind speed and gust time scale. In addition the method offers to embed the resulting extreme wind gust consistently in a (coherent) stochastic wind field. Based on measured data, extracted from "Database on Wind Characteristics" (http://www.winddata.com/), the method has been applied to estimate the magnitudes of wind speed gusts with similar shape, time extend and return period as the gusts specified in the IEC 61400-1 code. The estimated extreme gust amplitudes from the analysis shows substantial qualitative and quantitative differences compared to the specifications in the most recent IEC-61400 code revision. The third contribution concerns a re-calibration of the EOG load case in the IEC-61400 code. Assuming the mean wind speed to be Rayleigh distributed (as specified in the code) and adopting the conjecture that wind speed gust amplitudes scale directly with the turbulence standard deviation, the EOG amplitudes have been estimated for the 3 WTGS classes combined with the 3 turbulence classes prescribed in the IEC-61400 code. The estimation is performed for recurrence periods 1 year and 50 years, respectively, and the estimated amplitudes are finally synthesised into a simple algebraic expression.

The question of extreme shear is treated in two contributions. The first contribution concerns a rational evaluation of specifications, as given in the IEC 61400-1 code, for short-term extreme wind shear loading. The evaluation is based on wind speed measurements extracted from the "Database on Wind Characteristics" (www.winddata.com). Distributions for positive, as well as negative, extreme wind shear events (conditioned on the mean wind speed) are determined and subsequently compared for a number of offshore sites. In the second contribution, three different averaging periods (2, 5 and 10 seconds) are considered for a range of offshore locations. For each averaging period a relation between the resulting extreme shear distributions and the averaging time are presented. This short-term extreme shear analysis is based on different spatial distances, and extrapolation to a spatial distance of 100 m has been investigated. Finally, the most likely offshore short-term extreme shear values are estimated and subsequently compared with the values specified in the IEC-61400 code.

4.1 Statistics of offshore wind speed gusts

Gunner Chr. Larsen[1] and Kurt S. Hansen[2]
[1] Risø National Laboratories, Wind Energy Department, P.O. Box 49, DK-4000 Roskilde; E-mail: gunner.larsen@risoe.dk
[2] Department of Mechanical Engineering, Technical University of Denmark, DK-2800 Lyngby; E-mail:ksh@mek.dtu.dk

ABSTRACT: The present paper deals with a statistical method that, based on experimental observations, can be applied to estimate the probability density function for extreme events corresponding to an arbitrary recurrence period.
The statistical approach is described and subsequently applied on data sets representing wind speed gusts originating from two off shore locations with different characteristics. Upstream fetch and water depth are known to be leading parameters in relation to off shore wind climate characteristics, and the off shore sites selected for the present investigation represent coastal ocean waters as well as more constrained inner Danish waters. The analysis are based on measurements extracted from "Database on Wind Characteristics" (http://www.winddata.com/), where more than 72000 hours of high quality wind field data, representing a wide variety of wind climates and terrain types, are available.
The estimated extreme distributions associated with the investigated off shore sites are mutually compared, and finally the most likely extremes, derived from the estimated distributions, are compared to the IEC 61400-1 specifications associated with turbulence class B.

Keywords: Coastal Sea Areas, Extreme Wind Conditions, Gust Models, Off-Shore, Statistical Analysis, Turbulence

1 INTRODUCTION

Verification of the structural integrity of a wind turbine involves analysis of fatigue loading as well as ultimate loading. With the trend of persistently growing turbines, the ultimate loading seems to become relatively more important. For wind turbines designed according to the wind conditions prescribed in the Draft IEC 61400-1 standard (safety requirements) [1], the ultimate load is often identified as the leading load parameter.

The specifications in the IEC 61400-1 code are applicable to onshore siting only. However, taken into account the planned huge development of off shore wind energy in for example Denmark, a more detailed knowledge on the off shore design ultimate loads become of vital importance. Extreme wind speed gusts are a type of ultimate loading that may be critical for the structural integrity of a wind turbine.

2 STATISTICAL METHODOLOGY

The occurrence of gusts (and thus gust extremes), with limited time scale, within recordings of the wind speed is a result of the stochastic nature of turbulence. It is well known (and intuitively clear) that the amplitude of such gusts is closely related to the standard deviation associated with the stochastic process that describes the wind speed [2].

As the wind speed standard deviation is known to depend strongly on the mean wind speed[3], the statistics of extreme gust excursions is also likely to depend on the mean wind speed. As a result, the statistical analysis to be outlined in the following involves statistics conditioned on the mean wind speed.

2.1 Conditional Extreme distributions

At a given site and in a given height above the water surface, we now consider N samples each of size n (which are typically the number of wind speed gust observations within a time span of 10 minutes) taken from the same population. Referring to the above discussion, we assume the population to be uniquely *defined* by the mean wind speed associated with each sample.

An extreme value distribution can now be established based on the largest value taken from each sample. The distribution of the largest value among N observations must asymptotically approach the distribution of the largest value within samples of size n, provided that an asymptotic distribution exists. An extreme value distribution, EV1, satisfying these requirements can be derived [4], and initially we will *assume* that the observed wind speed gust extremes, conditioned on the mean wind speed, can be described by this statistical distribution.

The extremes, conditioned on the mean wind speed, will thus be distributed according to a cumulative probability density (CDF) function with two parameters of the form:

$$F_{eg}(x;\alpha,\beta_{eg}|U) = \exp(-\exp(-\alpha(x-\beta_{eg}))), \tag{1}$$

where U denotes the mean wind speed over the sampling period, and α, β_{eg} are the distribution parameters. The associated probability density function (PDF), conditioned on the mean wind speed, is given by:

$$f_{eg}(x;\alpha,\beta_{eg}|U) = \alpha\exp(-\exp(-\alpha(x-\beta_{eg})))\exp(-\alpha(x-\beta_{eg})) \tag{2}$$

Note, that the distribution parameters in general will depend on the mean wind speed, because this parameter defines the population of observations.

2.2 Unconditional Extreme Statistics

The conditional extreme statistics, associated with a given observation time, can now be used to establish the extreme statistics for an arbitrary recurrence period T.

The first step is to determine an unconditional extreme distribution, f_{uc}, corresponding to an arbitrary population, but still based on the basic sample length (typically corresponding to a 10-minute observation time). As the population is assumed to be uniquely defined by the mean wind speed, the unconditional EV1 distribution is obtained as a weighted mean of the conditional EV1 distributions over all possible populations. The applied weight reflects the probability of a given population. Thus:

$$f_{uc}(x;k,\beta_U) = \int_0^\infty f_{eg}(x;\alpha,\beta_{eg}|U)\, f_U(U;k,\beta_U)\, dU\ . \tag{3}$$

The mean wind speed is conventionally *assumed* to follow a (two parameter) Weibull distribution, given by the following CDF and PDF, respectively:

[3] For onshore sites (constant roughness length), the wind speed standard deviation is roughly proportional to the mean wind speed, whereas for off shore sites the wind speed standard deviation will increase more rapidly with the wind speed, as the sea roughness (caused by the waves) increases with increasing mean wind speed.

$$F_U(U;k,\beta_U) = 1 - \exp\left[-\left(\frac{U}{\beta_U}\right)^k\right] \;;\; U \geq 0\,, \tag{4}$$

$$f_U(U;k,\beta_U) = \frac{k}{\beta_U}\left(\frac{U}{\beta_U}\right)^{k-1} \exp\left[-\left(\frac{U}{\beta_U}\right)^k\right] \;;\; U \geq 0\,, \tag{5}$$

where U denotes the mean wind speed, and k, β_U are the (shape and intensity) distribution parameters.

The second and last step is to utilise the above unconditional extreme gust distribution, associated with a basic (for example 10-minute) return period, in a Monte Carlo simulation to establish the extreme gust statistics for an arbitrary return period. In addition to determination of the extreme distribution, the Monte Carlo technique also provides information on the mean wind conditions (the conditioned distributions) that contribute most significantly to the resulting extreme distribution.

Based on the extreme gust distribution, associated with a return period of one year, the most likely size of the one-year and fifty-year extreme gust is determined. The most likely fifty-year extreme value is defined as the one-year extreme, which in average occurs only once in a fifty-year period, thus corresponding to the 98% quantile in the one-year extreme distribution.

3 DATA MATERIAL

The method described in Section 2 has been applied to analyse wind speed gust events originating from two off shore locations with different characteristics. Upstream fetch and water depth are known to be leading parameters in relation to off shore wind climate characteristics, and therefore the off shore sites selected for the present investigation represent coastal ocean waters (Horns Rev) as well as more constrained inner Danish waters (Vindeby).

3.1 Vindeby

The Vindeby site is located off the north-western coast of Lolland in Denmark on a shallow water area with water depths ranging between 2.1m and 5.1m. The analysed measurements originated from a meteorological mast erected at a position with a minimum distance to land equal to 1270m.

Only cup anemometer recordings from the maximum level (45m) are investigated, as this level is close to the hub height for a modern wind turbine. Further, the data material is restricted to the mean wind direction sector 216°-339° in order to obtain a pure sea fetch free from mast- and boom effects. The present sea fetch is characterised by having more than 15 km of sea upstream [5]. With the defined selection criteria, the available data material constitutes 5615 10-minute time series with mean wind speeds ranging up to approximately 20m/s supplemented with 250 days of resource measurements.

3.2 Horns Rev

The Horns Rev site is located off the western coast of Jutland in Denmark on a reef with water depths ranging between 6m and 12m. Around the reef the water depths are somewhat larger. The available measurements originate from a 62m high meteorological tower erected a position with the distance to land exceeding 18.6km in all directions.

Only sonic recordings from the 50m level are investigated, as this level is almost identical with the recording level associated with the selected Vindeby measurements. The analysed recordings are not restricted to any particular mean wind direction sector, and the available

data material is thus constituted by 9737 10-minute time series with mean wind speeds ranging up to 20.5m/s supplemented with approximately 660 days of resource measurements.

4 DATA ANALYSIS

First step is to define a wind speed gust. In the present context a wind speed gust is defined as the difference in wind speed associated with a given temporal separation – here 5 seconds. Using consecutive time windows of length 5 seconds, each time series (of equal time span – here 10 minutes) defines a sample consisting of all identifies wind speed gusts within the particular wind speed time series.

In order to establish the conditional extreme distributions, the identified samples are categorised in 10-minute mean wind speed bins. The width of the mean wind speed bins is a compromise between a suitable mean wind speed resolution and the number of resultant extreme gust events available for the statistical fits. In the present analysis, the available mean wind speed ranges have been subdivided into 4 data categories defined by having mean wind speeds in the ranges 5-9 m/s, 9-13 m/s, 13-18 m/s and above 18 m/s, respectively. Hence only extreme gust events associated with mean wind speeds above 5 m/s are considered relevant for the overall extreme wind speed gust distribution. For each data category, the mean of the respective 10-minute mean wind speeds is used to characterise the bin.

For each mean wind bin, the conditional extreme gust distribution is determined by plotting the observed (extreme) gust values in an EV1 depiction, and subsequently derive the distribution parameters from a linear least square fit to these observations. For an ideal EV1 distributed variable, the EV1 depiction results in a linear relationship. It is characteristic that the present data material results in a very close to linear behaviour, thus confirming the assumption of the present extreme gust events being approximately EV1 distributed. An example of an EV1 depiction of extreme gust events, originating from the Vindeby site, is given in Figure 1.

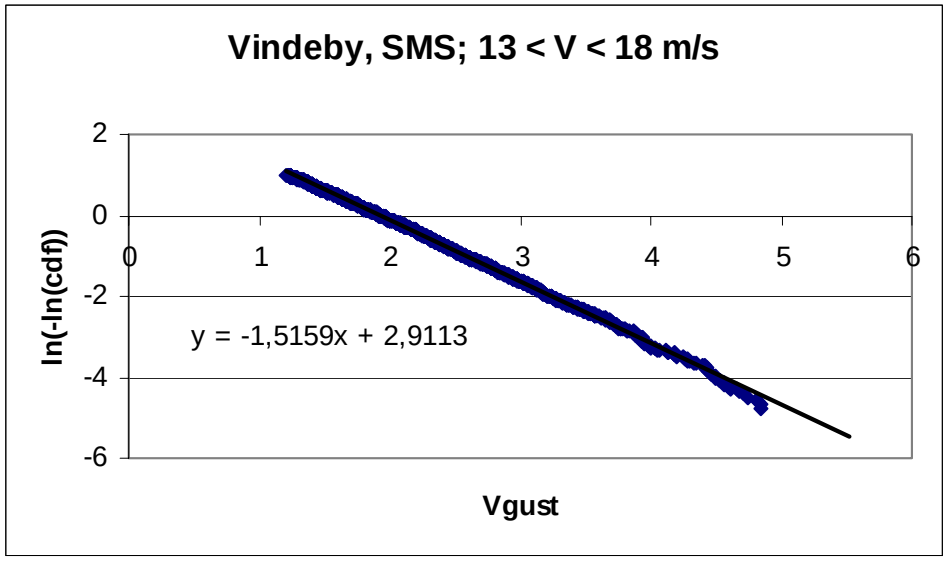

Figure 1: EV1 depiction of extreme gust events.

Having evaluated the parameters in the extreme distributions, conditioned on the mean wind speed, the variation of these with the mean wind speed is estimated by the following procedure. The distribution parameter values (related to the mean wind speeds characterising the selected bins) are initially transformed to distribution means and distribution standard

deviations, which are then subsequently fitted to a second order polynomial in the mean wind speed. Finally, the inverse of the above transformation is applied to yield the relationship between the distribution parameters and the mean wind speed. The applied fitting procedure has shown to be robust for the present data material, and has in addition the advantage of implicitly ensuring values of the α-parameter obeying the distribution requirement of being positive.

Note, that the estimated relationships are used to extrapolate beyond the parameter range covered by the available data material when evaluating the unconditional distribution given by equation (3). This inevitable introduces some uncertainty. On the other hand, however, the convolution of the conditional distributions with the Weibull distribution assures only a limited influence from extreme events occurring at extreme mean wind speeds. The fitted relationships for the distribution parameters, associated with the Vindeby data material, are shown in Figures 2 and 3.

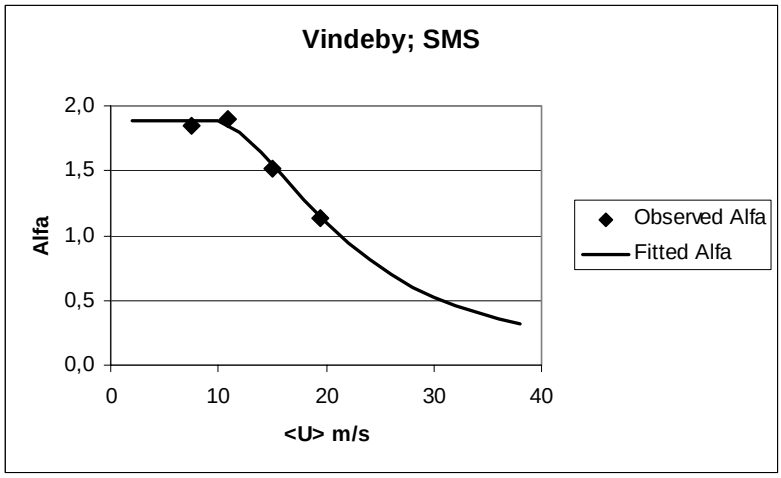

Figure 2: Fit of the α-parameter variation with the mean wind speed.

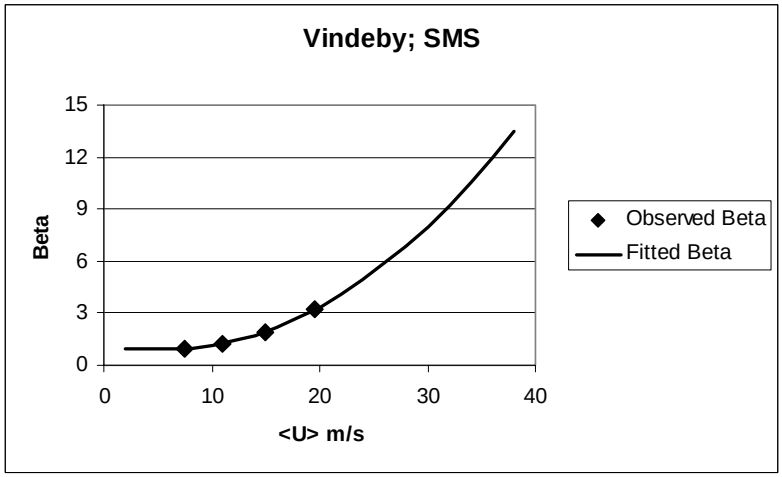

Figure 3: Fit of the β-parameter variation with the mean wind speed.

In order to determine the unconditional extreme gust distribution, the Weibull distribution of the mean wind speed must be estimated. The estimation is based on the available resource data, and it is performed utilising a Weibull depiction. In analogy with the EV1 distribution analysis, the Weibull parameters are uniquely derived from a linear fit in the performed

depiction.

The final step in the analysis is to synthesise the estimated EV1 distribution parameter dependence with the mean wind speed and the estimated Weibull parameters in a Monte Carlo simulation to obtain the unconditional extreme gust distribution for return periods equal to one and fifty years, respectively. In the present analysis, the extreme distributions are established performing Monte Carlo simulations over 30.000 years in order to ensure satisfactory convergence of the statistics.

5 RESULTS

The estimated extreme gust distributions associated with recurrence periods equal to one year and fifty years, respectively, are shown in Figures 4 and 5 for the two investigated off shore sites. There is a small difference in recording level between the two sites. However, a detailed investigation of the (average) wind shear profiles[4] indicates that the effect on the mean wind speed is less than 1%. The difference in observation height is therefore also considered neglectable in relation to gust events, and a direct comparison of the estimated distributions is consequently meaningful.

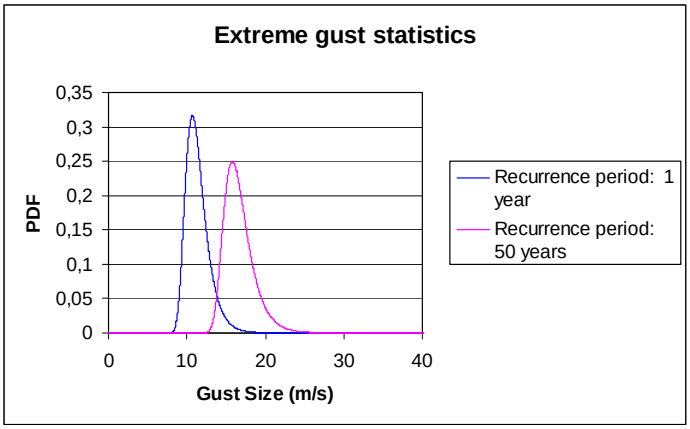

Figure 4: **Estimated extreme gust distributions at the Vindeby site.**

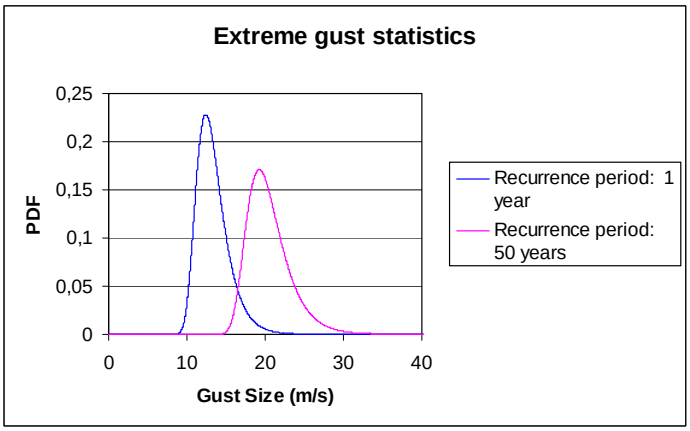

Figure 5: Estimated extreme gust distributions at the Horns Rev site.

The most likely extreme gusts, with a recurrence period of one year, can thus be estimated to 10.7m/s and 12.4m/s for the Vindeby and the Horns Rev site, respectively. The most likely extreme gusts, with a recurrence period of fifty years, are estimated to 15.8 m/s and 19.2m/s, respectively.

[4] Adopting a power law formulation, the exponent is estimated to 0.11.

A detailed comparison of the distributions, associated with the two sites, shows that the Horns Rev site is characterised by having conditional extreme gust amplitude distributions with smaller mean values than the conditional extreme gust distributions observed for the Vindeby site. This result may be explained by the fact that shallow water conditions tend to generate larger roughness than (coastal) ocean waters due to the more frequent occurrence of small and steep waves. On the other hand, the Weibull distributions for the observed 10-minute mean wind speed values suggests that large mean wind speeds are slightly more frequent[5] at the Horns Rev site compared to the Vindeby site, which, other things being equal, will favour the occurrence of larger gusts. The estimated one-year and fifty-year extreme gust distributions combine these two opposite directed effects.

The Monte Carlo method provides additional information on what mean wind speeds that contribute to the resulting extreme distributions. It turned out that only mean wind speeds up to approximately 31m/s contribute to the Vindeby extreme gust distribution, whereas mean wind speeds up to 37m/s contribute to the Horns Rev distribution. This is in accordance with the observed smaller shape factor in the Weibull distribution associated with the Horns Rev site.

For both sites wind speeds in the interval 5m/s to 50m/s have been considered in the Monte Carlo simulation. The lack of extreme gust contributions from very large mean wind speed regimes is due to the rapid decrease of the Weibull distribution for these large mean wind speeds.

Now, turning to the one-year and fifty-year extreme (operating) gust amplitudes as prescribed in the IEC 61400-1 code[6], the extreme operating gust amplitudes, for a 42m diameter wind turbine operating at 25m/s, equal 14.4m/s and 19.2m/s, respectively. The gusts prescribed in the code are thus conservative compared to the estimated most likely extreme gusts at the two investigated off shore sites. However, for a fifty-year recurrence period, the Horns Rev estimate equals the code specification.

6 CONCLUSION

A method to estimate extreme gust amplitude distributions, with arbitrary recurrence periods, has been presented. The method has subsequently been used to estimate extreme gust distributions for two off shore sites with different wind characteristics - a coastal ocean water site and a shallow water site located in more constrained inner Danish waters.

It has been demonstrated that, although the shallow water site is exposed to larger water surface roughness, the more frequent occurrence of large mean wind speeds at the coastal ocean site more than compensate for this regarding generation of extreme wind speed gusts. The most likely extreme gusts, at the coastal ocean site, exceed the most likely extreme gusts, at the shallow water site, with 16% and 22% (for a one-year and a fifty-year recurrence period), respectively. The 61400-1 code specifications have been demonstrated to be conservative.

The present investigation is based purely on measurements, but the applied methodology can easily include additional data originating from turbulence simulations, covering wind speed ranges where experimental results are lacking. Such a strategy can potentially improve the accuracy of the extreme gust distribution estimates.

7 REFERENCES

[5] The mean wind speed distributions for the two sites have approximately the same mean value, but the Weibull shape parameter is less for the Horns Rev site yielding enhanced probability of large mean wind speeds compared to the Vindeby site.

[6] Turbulence class B is assumed.

[1] IEC 61400-1 Wind Turbine Safety System: part 1, Safety Requirements.
[2] Newgust; Final report.
[3] Database on Wind Characteristics. http://www.winddata.com/.
[4] Gumbel, E.J.; Statistics of Extremes (1966). Columbia University Press.
[5] Barthelmie, R.J. et. al. (1994). The Vindeby Project: A Description. Risø-R-741.

4.2 Constrained simulation of critical wind speed gusts by means of wavelets

Gunner Chr. Larsen[1], Kurt S. Hansen[2], and Bo Juul Pedersen[3]
[1] Risø National Laboratories, Wind Energy Department, P.O. Box 49, DK-4000 Roskilde; E-mail: gunner.larsen@risoe.dk
[2] Department of Mechanical Engineering, Technical University of Denmark, DK-2800 Lyngby; E-mail:ksh@mek.dtu.dk
[3] NEG-Micon A/S, Alsvej 21, DK-8900 Randers, Denmark; E-mail: bjp@neg-micon.dk

ABSTRACT: For most structures exposed to wind loading, extreme response is associated with extreme wind speeds. However for wind turbines - especially *for pitch regulated* wind turbines - the design driving *thrust* loading is often associated with severe wind gust situations occurring during normal operation and these are thus related to the mean wind speed regime [5m/s; 25m/s].
Based on knowledge on the load response characteristic of the wind turbine (in terms of aerodynamics and pitch action) it is possible to identify a general critical mean gust shape that may potentially result in ultimate thrust loading. In the IEC 61400-1 design code, this particular load case is defined as Extreme Operational Gust (EOG). This (coherent deterministic) gust has a characteristic "Mexican hat" shape with prescribed time extend and magnitude. The time constant depends on the return period of the extreme wind speed gusts, whereas the magnitude depends on the return period as well as the mean wind speed.
The present paper presents a rational method to calibrate the wind speed gust magnitudes specified in the IEC 61400-1 code. The method combines a wavelet expansion with extreme statistics and results in consistent estimates of wind speed gust magnitudes for arbitrary return period, mean wind speed and gust time scale. In addition the method offers to embed the resulting extreme wind gust consistently in a (coherent) stochastic wind field.
Based on measured data, extracted from "Database on Wind Characteristics" (http://www.winddata.com/), the method has been applied to estimate the magnitudes of wind speed gusts with similar shape, time extend and return period as the gusts specified in the IEC 61400-1 code.

Keywords: Extreme Statistics, Extreme Wind Conditions, Gust Models, Turbulence, Wind Speed Gusts.

1 INTRODUCTION

Verification of the structural integrity of a wind turbine according to the Draft IEC 61400-1 code [1] involves analysis of a number of ultimate load cases. Among these is the load case Extreme Operational Gust (EOG), which is of particular relevance for the thrust loading of pitch regulated wind turbines due to its characteristic "Mexican hat" like shape. The EOG load case is a coherent deterministic gust with prescribed time scale and magnitude.

The present paper presents a rational method to calibrate the wind speed gust magnitudes specified in the IEC 61400-1 code. In addition the method offers to embed the resulting extreme wind speed gust consistently in a (coherent) stochastic wind field.

2 METHODOLOGY

The method is based on identification of gust occurrences of the prescribed shape and time scale in full scale measurements, followed by an extreme-value analysis of the identified gust magnitudes. The extreme-value analysis encompasses transformation of the estimated extreme gust magnitudes to return periods others than the available recording periods. Finally, the method allows for embedding the resulting extreme gusts in a (coherent) stochastic wind field that can be used as input to aeroelastic simulations of wind turbine response.

2.1 Wavelet transformation

Wind speed gust phenomena are typically characterised by having compact support is the time domain as well as in the frequency domain. As a consequence such wind situations are well suited for expansion in wavelets. Inspired by the EOG gust shape, the identification of gust occurrences in measured wind field time series is based on a wavelet expansion of the wind speed signal using the *Mexican hat* wavelet as a mother wavelet. The Mexican hat wavelet is equal to the second derivative of a Gaussian, whereas the EOG load case is expressed in terms of trigonometric functions. However, both formulations are idealisations of a critical wind speed gust shape occurring as realisations in a stochastic field, and the conceptual difference between these is therefore not considered important in the present context.

The Mexican hat wavelet is expressed [6] as:

$$\psi(t) = \frac{1}{\sqrt{\Gamma(5/2)}}\left(1-t^2\right)e^{-t^2/2}. \tag{1}$$

Basically, a wavelet function must satisfy the weak *admissibility condition* formulated as:

$$C\psi = \int_0^\infty \frac{|\hat{\psi}(\omega)|^2}{\omega} d\omega < \infty \ , \tag{2}$$

where $\hat{\psi}(\omega)$ is the Fourier transform of $\psi(t)$.

As a consequence of equation (2) the DC component must equal zero, from which it is seen that a wavelet function must have zero mean. Associated with the mother wavelet is a family of time-frequency "atoms" obtained by scaling and translating the mother wavelet by *s* and *u*, respectively. In the process of scaling the mother wavelet function, the energy of the scaled wavelets must be kept constant. This is achieved by suitable normalisation, and the resulting wavelet functions are expressed by:

$$\psi_{u,s}(t) = \frac{1}{\sqrt{s}}\psi\left(\frac{t-u}{s}\right) \ . \tag{3}$$

Note, that the wavelet functions expressed by equation (1) and (3) are normalised such that

$$\left\langle \psi_{u,s}, \psi_{u,s} \right\rangle \equiv 1 \ , \tag{4}$$

where $\langle *,* \rangle$ denotes the inner product.

The wavelet transform of a signal, *f(t)*, is a convolution product given by:

$$W_\psi f(u,s) = \left\langle f, \psi_{u,s} \right\rangle = \int_{-\infty}^{\infty} f(t)\frac{1}{\sqrt{s}}\psi^*\left(\frac{t-u}{s}\right)dt \ , \tag{5}$$

where $*$ denote complex conjugate. A given wavelet coefficient "measures" the correlation of the signal with the particular wavelet. As the Mexican hat wavelet has compact support in the

time as well as in frequency, it measures the variations - in the frequency band corresponding to the scale parameter *s* - of *f(t)* in the neighbourhood of *u*.

With wavelet functions obeying the *admissibility condition*, it is possible to reconstruct the original signal from its wavelet transform as [6]

$$f(t)=\frac{1}{C_\psi}\int_0^\infty\int_{-\infty}^{\infty} W_\psi f(u,s)\frac{1}{s^{5/2}}\psi\left(\frac{t-u}{s}\right)duds \ . \tag{6}$$

Note, that equation (6) is true even when the wavelet atoms do not form an orthogonal basis. This is the situation for the Mexican hat wavelet, and the consequence is that some redundant information is hidden in the computed wavelet coefficients.

The constant C_ψ can be analytically determined from equation (2), and we have the following identity [5]:

$$C_\psi \equiv \frac{1}{2\Gamma(5/2)} \ . \tag{7}$$

Referring to the EOG load case, the focus is on a coherent wind speed signal, *v(t)*, of the form

$$v(t)=\frac{A}{\sqrt{s_0}}\psi\left(\frac{t-u_0}{s_0}\right)+g(t) \ , \tag{8}$$

where *A* is a normalised amplitude, s_0 denotes the wavelet scale corresponding to the requested time extend of the gust, u_0 is the position of gust on the time axis, and *g(t)* is a stochastic (turbulence) process superimposed on the gust signal.

Let us now apply the wavelet transformation, expressed in equation (5), on the wind speed signal given by equation (8). Thus

$$W_\psi v(u,s)=A\left\langle\psi_{u_0,s_0},\psi_{u,s}\right\rangle+\left\langle g,\psi_{u,s}\right\rangle \ . \tag{9}$$

The particular wavelet coefficient corresponding to scale s_0 and position u_0 is thus

$$W_\psi v(u_0,s_0)=A\left\langle\psi_{u_0,s_0},\psi_{u_0,s_0}\right\rangle+\left\langle g,\psi_{u_0,s_0}\right\rangle \ . \tag{10}$$

For sufficiently large amplitudes *A* the following approximation is valid

$$W_\psi v(u_0,s_0)\approx A\left\langle\psi_{u_0,s_0},\psi_{u_0,s_0}\right\rangle=A \ , \tag{11}$$

where the last identity is obtained from equation (4).

Suppose, we want to modify the wind field given by equation (8) in the sense that the amplitude *A* is to be replaced by an amplitude *nA*, where n is some (known) factor. The modified wind speed signal, $v_m(t)$, is thus given by

$$v_m(t)=\frac{nA}{\sqrt{s_0}}\psi\left(\frac{t-u_0}{s_0}\right)+g(t) \ . \tag{12}$$

The wavelet coefficients corresponding to the modified signal is given by

$$W_\psi v_m(u,s)=nA\left\langle\psi_{u_0,s_0},\psi_{u,s}\right\rangle+\left\langle g,\psi_{u,s}\right\rangle \ . \tag{13}$$

Combining equations (10) and (11), a relation between the wavelet coefficients corresponding to the original wind speed signal and the modified wind speed signal, respectively, is obtained as

$$W_\psi v_m(u,s) = W_\psi v(u,s) + (n-1)A\langle \psi_{u_0,s_0}, \psi_{u,s} \rangle \quad . \tag{14}$$

The inner product in the last term of equation (14) is simply the reproducing kernel of the wavelet. It measures the correlation of arbitrary two wavelet atoms, and is a quality with the applied wavelet and as such independent of the analysed signal. For the Mexican hat wavelet, the reproducing kernel can be evaluated analytically. The computations, as well as the result, is somewhat lengthy, and is therefore not reproduced here - we refer to reference [5]. The interpretation of equation (14) is that a wavelet expansion of the modified wind speed signal, obtained by increasing the gust amplitude from *A* to *nA*, can be obtained by extracting the influence from the original gust on the wavelet coefficients, and subsequently introduce the influence from the modified gust in the wavelet coefficients. Note, that a prerequisite for this transformation is knowledge to the amplitude *A*, and thus (from equation (11)) the existence of sufficiently large gusts with the prescribed characteristics in the data material.

Having modified the wavelet coefficients according to equation (14) the associated time series representation is obtained applying the inverse wavelet transformation, as given in equation (6), on the modified wavelet coefficients. Note, that (knowing the initial amplitude *A*) the amplitude of the modified gust equals *nA* (cf. equation (12)).

The basic idea in the present paper is to identify large values of the amplitude *A*, from a large number of full scale wind field measurements, by means of wavelet filtering as described above. These gust amplitudes will refer to a limited return period typically given by the length of the available time series records. By use of extreme-value statistics, the most likely gust amplitudes for arbitrary return periods can be estimated and then subsequently introduced in a coherent wind field using the method summarized in equations (14) and (6).

2.2 Extreme statistics

The occurrence of wind speed gusts (and thus gust extremes), with limited time scale is a result of the stochastic nature of turbulence. It is well known (and intuitively clear) that the amplitude of such gusts is closely related to the standard deviation associated with the stochastic process that describes the wind speed [2].

As the wind speed standard deviation is known to depend strongly on the mean wind speed, the statistics of extreme gust excursions is also likely to depend on the mean wind speed. As a result, the analysis to be outlined in the following involves statistics conditioned on the mean wind speed.

At a given site and in a given height above the surface, we now consider N samples each of size n (which is typically the number of wavelet coefficients corresponding to the prescribed gust time scale within a record time span T) taken from the same population. Referring to the above discussion, we assume the population to be uniquely *defined* by the mean wind speed associated with each sample.

An extreme value distribution can now be established based on the largest value taken from each sample. The distribution of the largest value among N observations must asymptotically approach the distribution of the largest value within samples of size n, provided that an asymptotic distribution exists. An extreme value distribution, EV1, satisfying these requirements can be derived [4]. Initially we will *assume* that the (extreme) computed wavelet coefficients with the requested characteristics, conditioned on the mean wind speed, can be described by this statistical distribution.

The extremes, conditioned on the mean wind speed, will thus be distributed according to a cumulative probability density (CDF) function with two parameters of the form:

$$F(W_\psi v; \alpha, \beta | U) = \exp\left(-\exp\left(-\alpha\left(W_\psi v - \beta\right)\right)\right) \quad , \tag{15}$$

where U denotes the mean wind speed over the sampling period, and (α, β) are the distribution parameters. The scaling and position parameters of the wavelet coefficients have been omitted for convenience. The associated probability density function (PDF), conditioned on the mean wind speed, is given by:

$$f\left(W_\psi v;\alpha,\beta|U\right)=\alpha\exp\left(-\exp\left(-\alpha\left(W_\psi v-\beta\right)\right)\right)\exp\left(-\alpha\left(W_\psi v-\beta\right)\right) \tag{16}$$

Note, that the distribution parameters in general will depend on the mean wind speed, because this parameter defines the population of observations.

The distribution parameters are estimated using a least square fit in the well established normal score plot depiction [5]. Having estimated the EV1 distribution, corresponding to the return period T, the extrapolation to an (arbitrary) other return period, pT, are performed based on an independence assumption in a binomial process. The resulting modified extreme value distribution, F_p, is thus determined from

$$F_p\left(W_\psi v;\alpha,\beta|U\right)=\left[F\left(W_\psi v;\alpha,\beta|U\right)\right]^p \ . \tag{17}$$

The extreme value with a return period equal to pT is the extreme value that *in average* is exceeded only once during the time span pT, thus corresponding to the (1-1/p) quantile in the extreme value distribution F expressed in equation (15). It can be shown [5] that, for the EV1 distribution, the (1-1/p) quantile in F corresponds (for large p) to the mode (i.e. the most likely extreme value) in the F_p distribution.

The value of p is related to a distribution conditioned on the mean wind speed. Usually, p is determined by initially selecting a return period corresponding to the overall wind climate on the site - i.e. typically the number of years to be considered. Based on knowledge to the mean wind climate on the site p is easily computed for selected mean wind speed bins. The mean wind speed is conventionally *assumed* to follow a (two parameter) Weibull distribution given by the following CDF and PDF, respectively:

$$\begin{aligned} F_U(U;k,\beta_U) &= 1-\exp\left[-\left(\frac{U}{\beta_U}\right)^k\right] \ ; \ U\geq 0 \ , \\ f_U(U;k,\beta_U) &= \frac{k}{\beta_U}\left(\frac{U}{\beta_U}\right)^{k-1}\exp\left[-\left(\frac{U}{\beta_U}\right)^k\right] \ ; \ U\geq 0 \ , \end{aligned} \tag{18}$$

where U denotes the mean wind speed, and k, β_U are the (shape and intensity) distribution parameters, respectively.

3 DATA MATERIAL

The method described in Section 2 has been applied to analyse wind speed gust events originating from a site located in Oak Creek, near Tehachapi in California.

The experimental setup consists of two 80m high meteorological towers erected on a ridge in a complex mountainous terrain. Although the site is complex, the turbulence intensity is not exceptional as seen from Figure 1, where the mean turbulence intensity has been depicted as function of the mean wind speed at level 65m.

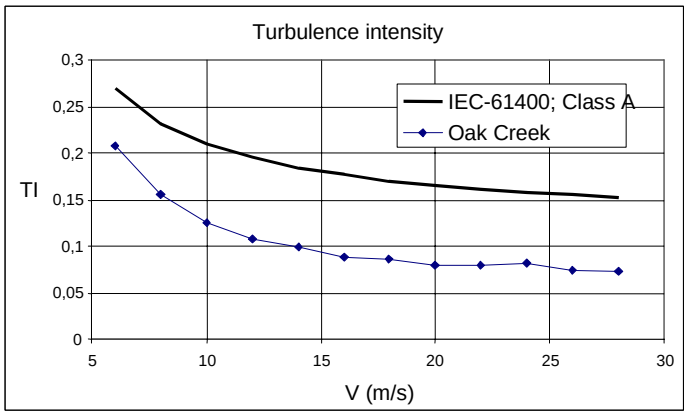

Figure 1: Turbulence intensity as function of mean wind speed at level 65m.

The meteorological towers are intensively instrumented with sensors in several heights above the ground surface. For the present investigation only cup anemometer recordings from the 65m level are applied, motivated by the fact that this level is close to the hub height for a modern wind turbine. The cup anemometer signal has been recorded with a sampling frequency equal to 8Hz.

The measurement campaign has been running from May 1998 until November 2000, and it has resulted in a large number of wind field time series covering a mean wind speed range extending from 0.5m/s to 29.4m/s. Of these 9506 10-minute time series have been selected covering the normal operational regime of a wind turbine. The recording system is designed to deliver an overrepresentation of time series with mean wind speeds above 15m/s, compared to a continuous recording strategy. This is an advantage for the present type of analysis based on extreme distributions conditioned on the mean wind speed, as it ensures a fair representation of events even in mean wind speed bins with representing high mean wind speeds.

4 DATA ANALYSIS

The first step is to identify occurrences of wind speed gusts, with prescribed characteristics concerning shape and time scale, using a filtering process based on a wavelet expansion.

4.1 Wavelet transformation

The IEC code operates with characteristic time scales for (coherent) wind speed gusts equal to 10.5s and 14.0s for gusts with recurrence periods of 1 year and 50 years, respectively. Initially, these time scales are transformed to characteristic wavelet scales. Referring to equation (3), we denote these s_1 and s_{50}, respectively.

Subsequently, a suitable discretization of the wavelet space is performed in terms of the scaling and translation parameters s and u (c.f. equation (3)). Care must be taken that s_1 and s_{50} are realised in the discretization of the scaling parameter s. For the discretization of the translation parameter u, it is important that the increments are small compared to the characteristic gust time scales in question. The reason is that the approximation expressed in equation (11) is best when, in the wavelet domain, the characteristic gust is resolved primary in one dominating wavelet coefficient.

With the selected discretization, the wavelet transformation is performed in accordance with the direction given in equation (5), except that the finite length character of the investigated time series implies that the integration interval is also of finite length. However, due to *the cone of influence* [6] for the support of a given wavelet atom, the integration interval must exceed the length of the analysed time series. For the present investigation, it

was, somewhat arbitrary, selected to extend the integration t-regime with 5*s* in both ends of the available wind speed time series. Within these 2×5*s* intervals a function value of zero has been assumed.

Having performed the wavelet transformation for all available time series, the wavelet coefficients with scales s_1 and s_{50} are extracted for a succeeding extreme value analysis.

4.2 Extreme statistics

Initially, the extracted wavelet coefficients are binned according to the mean wind speed of the wind speed time series they refer to. A step in bin size equal to 2m/s has been selected, and the wind speed regime outside the normal operation regime (5m/s<*U*<25m/s) of a wind turbine is excluded from the analysis. The width of the mean wind speed bins is as usual a compromise between a suitable mean wind speed resolution and the number of resulting extreme events available for performing the statistical fits.

For each time series, belonging to a particular mean wind speed bin, the largest wavelet coefficients (with scales s_1 and s_{50}, respectively) are identified and used as basis for the extreme value analysis, by fitting these to a (conditioned) distribution of the type given in equation (15). The fitting is performed by plotting the identified (extreme) wavelet coefficients in an EV1 depiction, and subsequently derive the distribution parameters from a linear least square fit to these observations. For an ideal EV1 distributed variable, the EV1 depiction results in a linear relationship. It is characteristic that the present data material results in a very close to linear behaviour, thus confirming the conjecture of the present extreme wavelet coefficients being approximately EV1 distributed. Representative examples of EV1 depictions of extreme wavelet coefficients for two different mean wind speed bins are given in Figure 2.

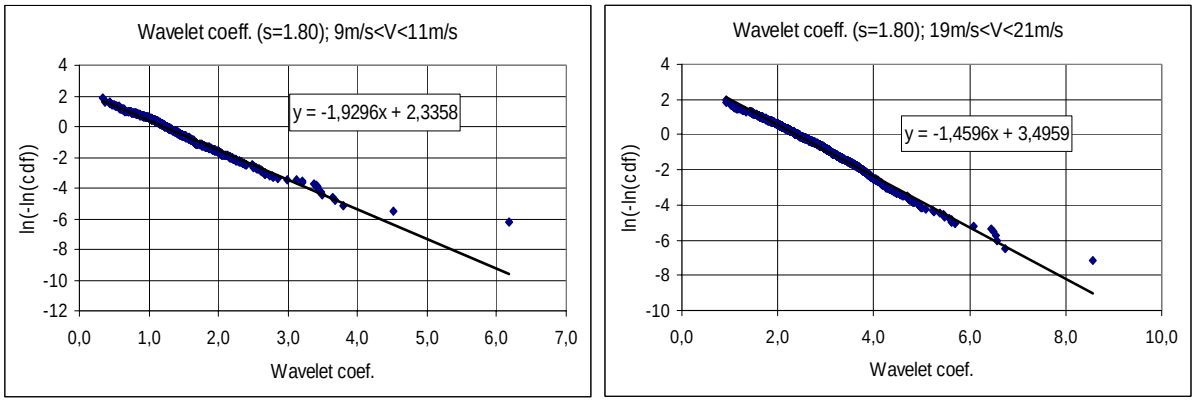

Figure 2: EV1 depiction of extreme wavelet coefficients corresponding to scale s_{50} .

With the estimated distribution parameters, the (conditional) extreme distributions of wavelet coefficients with scales s_1 and s_{50} are defined corresponding to a return period equal to the length of the investigated time series (10 minutes). A representative example of probability density functions (PDF) of extreme wavelet coefficients, related to the mean wind speed interval ranging between 9m/s and 11m/s are presented in Figure 3.

The last step, in the extreme value investigation of the selected wavelet coefficients, is to transform the estimated PDF's, referring to a return period equal to 10 minutes, to return periods of 1 year and 50 years, respectively. More specific, the PDF's of wavelets with scale s_1 is transformed to 1-year recurrence period distributions, whereas the PDF's of wavelets with scale s_{50} is transformed to 50-year recurrence period distributions. The transformation is performed in accordance with the method described in Section 2, assuming an IEC Class 1

site (annual mean wind speed equal to 10m/s) and a shape factor in the mean wind speed Weibull distribution (c.f. equation (18)) equal to 2, which makes it degenerate to the Rayleigh distribution applied in the IEC code.

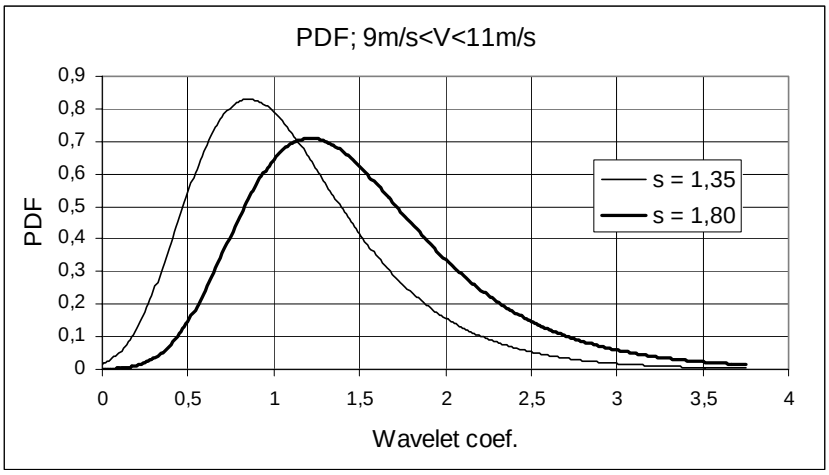

Figure 3: PDF of extreme wavelet coefficients with scales s_{50} and s_1, respectively.

5 RESULTS

The estimated extreme distributions of the selected wavelet coefficients associated with recurrence periods equal to one year and fifty years, respectively, have been used to estimate the *most likely* peak-peak value of IEC gusts with recurrence periods 1 year and 50 year, respectively. The peak-peak values are determined by combining the values of the most likely extreme wavelet coefficients with. equations (3) and (11). Note, that the estimated peak-peak values refer to the turbulence intensity level prevailing at the measuring site.

The estimated peak-peak values are subsequently compared with corresponding values obtained from the IEC code. The results for recurrence period 1 year and 50 years are shown in Figures 4 and 5, respectively.

It is characteristic that the IEC recommendations substantially over-estimate the observed extreme gust peak-peak values at the investigated site, when based on turbulence class A or B specifications.

However, if the standard turbulence description is replaced by the prevailing turbulence intensity at the present site, as given in Figure 1, the IEC recommendation turns out to under-estimate the estimated extreme gust peak-peak values.

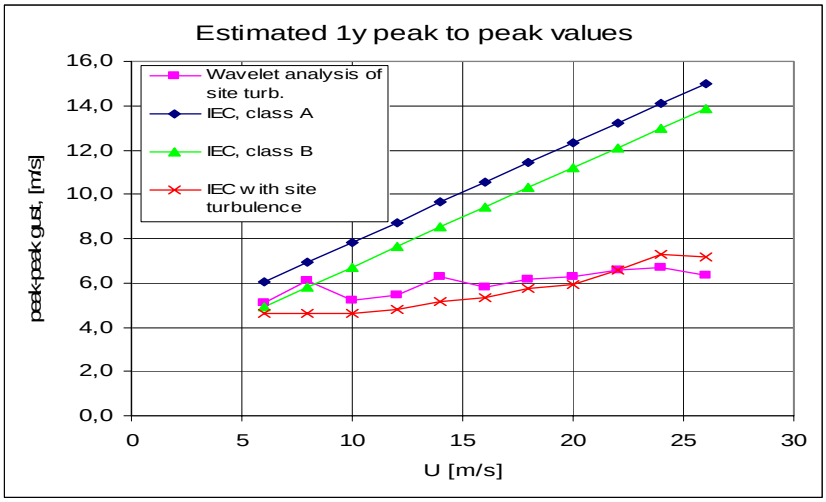

Figure 4: Gust peak-peak values (1 year).

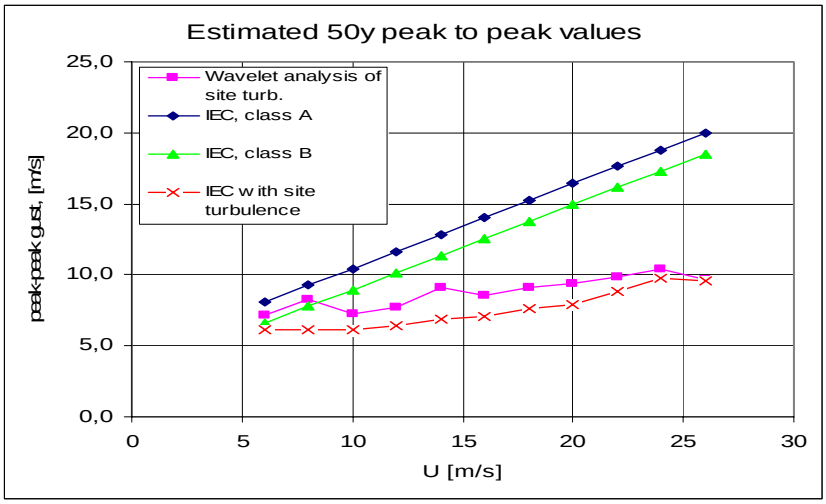

Figure 5: Gust peak-peak values (50 years).

In a conventional spectral turbulence description [1], the turbulence energy scales directly with the turbulence intensity squared. As a consequence, the turbulence velocity components scales directly with the turbulence intensity. Everything else kept constant this means that the gust amplitudes scales with the turbulence intensity. The consequence is that, for a given turbulence intensity, the IEC code tend to under-estimate the extreme gust peak-peak value for the EOG load case.

6 CONCLUSION

Based on a large number of one-point measurements, extreme (coherent) wind speed gust events with return periods 1 year and 50 years, respectively, have been estimated. For the relative large wind speed gust time scales investigated, it has thus implicitly been assumed that one-point gusts adequately represent fully coherent gusts over the rotor plane of a wind turbine. The gust estimates have subsequently been compared with predictions based on the IEC code. For *identical turbulence conditions*, the IEC code tend to somewhat under-predict the estimated extreme gust events, except for the high wind region associated with the return period 1 year.

Still outstanding are analyses of the criticality of other gust time scales as well as the sensibility of the estimated extreme gust events with the turbulence structure. More specific, the influence from Gaussian ctr. non-Gaussian turbulence behaviour, turbulence length scale and turbulence coherence characteristics should be investigated.

ACKNOWLEDGEMENT

The Danish Energy Agency funded the present work under the contract ENS 1363/01-0005.

7 REFERENCES

[1] IEC 61400-1 Wind Turbine Safety System: part 1, Safety Requirements.
[2] Bierbooms, W., Cheng, P.W., Larsen, G.C. and Pedersen, B.J. (2000). Modelling of Extreme Gusts for Design Calculations - NewGust. Publishable Final Report, TU Delft, Delft, The Netherlands.
[3] Database on Wind Characteristics. http://www.winddata.com/.
[4] Gumbel, E.J. (1966). Statistics of Extremes. Columbia University Press.
[5] Larsen, G.C., Pedersen, B.J. and Hansen, K.S.. Extreme coherent wind speed gusts. To appear.
[6] Mallat, S. (1998). A Wavelet Tour of Signal Processing. Academic Press.

4.3 On the most likely EOG amplitudes

Gunner Chr. Larsen[1] and Kurt S. Hansen[2]
[1] Risø National Laboratories, Wind Energy Department, P.O. Box 49, DK-4000 Roskilde; E-mail: gunner.larsen@risoe.dk
[2] Department of Mechanical Engineering, Technical University of Denmark, DK-2800 Lyngby; E-mail:ksh@mek.dtu.dk

ABSTRACT: For most structures exposed to wind loading, extreme response is associated with extreme wind speeds. However for wind turbines - especially *for pitch regulated* wind turbines - the design driving *thrust* loading is often associated with severe wind gust situations occurring during normal operation, and these are thus related to the mean wind speed regime [5m/s; 25m/s]. Based on knowledge on the load response characteristic of the wind turbine (in terms of aerodynamics and pitch action) it is possible to identify a general critical mean gust shape that may potentially result in ultimate thrust loading. In the IEC 61400-1 design code, this particular load case is defined as Extreme Operational Gust (EOG). The code prescribes the gust shape, extend and magnitude for recurrence periods 1 year and 50 years, respectively.
In a recent cogent study, based on wavelet filtering combined with extreme statistics, the *most likely* extreme amplitudes of wind speed gusts (with *shapes* and *time scales* identical to those specified for the EOG load case in the IEC-61400 code) have been assessed. The estimated extreme gust amplitudes from the analysis shows substantial qualitative and quantitative differences compared to the specifications in the most recent IEC-61400 code revision. Assuming the mean wind speed to be Rayleigh distributed (as specified in the code) and adopting the conjecture that wind speed gust amplitudes scale directly with the turbulence standard deviation, the EOG amplitudes have been estimated for the 3 WTGS classes combined with the 3 turbulence classes prescribed in the IEC-61400 code. The estimation is performed for recurrence periods 1 year and 50 years, respectively, and the estimated amplitudes are finally synthesised into a simple algebraic expression.

Keywords: Design Code, Extreme Wind Conditions, Gust Models, Turbulence, Wind Speed Gusts.

1 INTRODUCTION

Verification of the structural integrity of a wind turbine according to the Draft IEC 61400-1 code [2] involves analysis of a number of ultimate load cases. Among these is the load case Extreme Operational Gust (EOG), which is of particular relevance for the thrust loading of pitch regulated wind turbines due to its characteristic “Mexican hat” like shape. The EOG load case is a coherent deterministic wind speed gust with prescribed time scale and magnitude.

The present paper presents a rational method to calibrate the wind speed gust magnitudes specified in the IEC 61400-1 code. The calibration is performed for gust recurrence periods 1 and 50 years, respectively.

2 BACKGROUND

The occurrence of wind speed gusts (and thus gust extremes), with limited time scale is a result of the stochastic nature of turbulence. It is well known (and intuitively clear) that the

amplitude of such gusts is closely related to the standard deviation associated with the stochastic process that describes the wind speed [3].

In a recent cogent study [1], based on wavelet filtering combined with extreme statistics, the *most likely* extreme amplitudes of wind speed gusts (with *shapes* and *time scales* identical to those specified for the EOG load case in the IEC-61400 code) has been assessed for the Oak Creek site in USA. As the wind speed standard deviation is known to depend strongly on the mean wind speed, the statistics of extreme gust excursions in [1] has been evaluated conditioned on the mean wind speed.

The estimated extreme gust amplitudes from the study presented in [1] shows substantial qualitative and quantitative differences compared to the specifications in the most recent IEC-61400 code revision. For a WTGS Class I mean wind climate, the corresponding extreme gust amplitudes (corresponding to a one year recurrence period), as obtained from the investigation and the code, respectively, looks as reproduced in Figure 1.

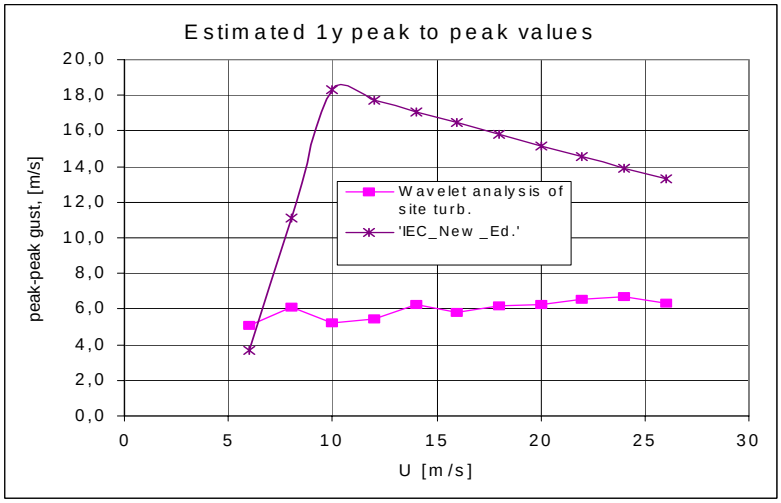

Figure 1: Most likely extreme gust amplitudes as function of the wind speed.

The observed significant differences between code specification and the results of the analysis performed in [1] can not be justified by the difference in turbulence level exclusively, as the turbulence intensity at the investigated site has a qualitative dependence with the mean wind speed comparable with the IEC-61400 code specifications as seen in Figure 2.

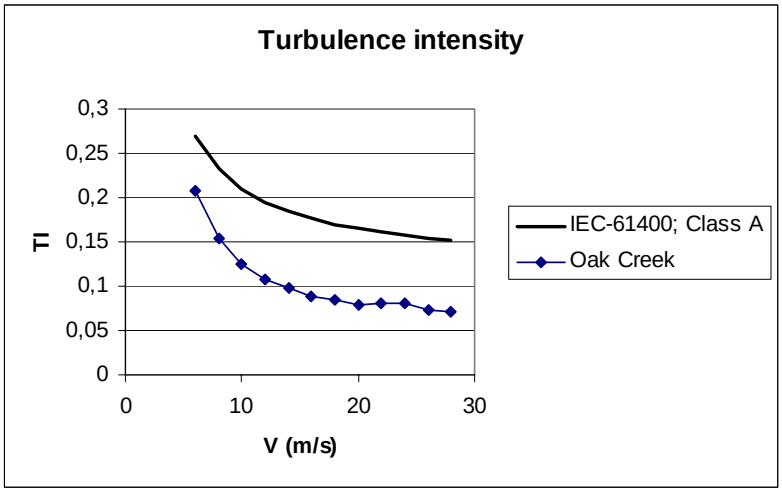

Figure 2: Turbulence intensities as function of mean wind speed.

3 ANALYSIS

The proposed EOG calibration method contains two steps: (1) a transformation of the "basic" conditional 10 minute extreme statistics from [1] to the requested recurrence periods in the IEC-61400 code, and (2) a transformation of the resulting most likely EOG amplitudes, corresponding to the turbulence intensity at the investigated site, to the most likely EOG amplitudes corresponding to the turbulence standard deviations as specified in the IEC code. The latter step ensures that the code turbulence intensity specifications are consistent with the code extreme amplitude specifications.

3.1 Transformation to requested recurrence periods

Basically, the analysis in [1] determines EV1 probability density functions (PDF's) of EOG gust amplitudes (with time scales as specified in the code), conditioned on the mean wind speed, and corresponding to a recurrence period equal to T=10 minutes. Assuming independence in a binomial type process, the transformation from a 10 minute recurrence period to 1 year and 50 year recurrence periods, respectively, is easily performed when the distribution of the mean wind speeds is known.

The extreme value with a return period equal to pT is the extreme value that *in average* is exceeded only once during the time span pT, thus corresponding to the (1-1/p) quantile in the extreme value distribution associated with the recurrence period T. For the EV1 distribution it can be shown [5] that the (1-1/p) quantile in the PDF, corresponding to recurrence period T, corresponds (for large p) to the mode (i.e. the most likely extreme value) in the PDF corresponding to a recurrence period equal to pT.

The value of p is related to a distribution conditioned on the mean wind speed. Usually, p is determined by initially selecting a return period corresponding to the overall wind climate on the site - i.e. typically the number of years, N, to be considered. Based on knowledge to the mean wind climate on the site, the value of p_i is easily computed for the individual mean wind speed bins (index i refers to the mean wind bin number).

Following the IEC-61400 code philosophy, the mean wind speed is *assumed* to follow a Rayleigh type cumulative distribution function (CDF):

$$F_U(U;\beta_U) = 1 - \exp\left[-\left(\frac{U}{\beta_U}\right)^2\right] \;;\; U \geq 0 \,. \tag{1}$$

In the analysis in [1], a mean wind speed bin size equal to ΔU=2m/s was selected, whereby p_i for the i'th mean wind speed bin is determined by

$$p_i = 52560N\left[F_U(U_i + \Delta U;\beta_U) - F_U(U;\beta_U)\right];\; U \geq 0 \,. \tag{2}$$

3.2 Transformation to code standard deviation

Central here is the adoption of the conjecture that the extreme wind speed gust amplitudes scale directly with the turbulence standard deviation. The present analysis focus on specific gust time scales (those specified in the IEC-61400 code for recurrence periods 1 and 50 years, respectively), which potentially might introduce a dependence of the extreme gust amplitudes on the turbulence length scale as well. However, the influence from the turbulence length scale is considered of second order importance and neglected in the present analysis.

4 RESULTS

The external load conditions to be considered, according to the IEC-61400 code, depend on the intended site for the wind turbine. The code specifies 3 representative mean wind classes that individually can be combined with 3 representative turbulence categories.

Using the method described in Section 3, the EOG amplitudes corresponding to the 9 standard wind climate conditions, emerging from combining the 3 mean wind classes with the 3 turbulence categories, are determined. The results are presented in Figures 3-8.

4.1 Recurrence period 1 year

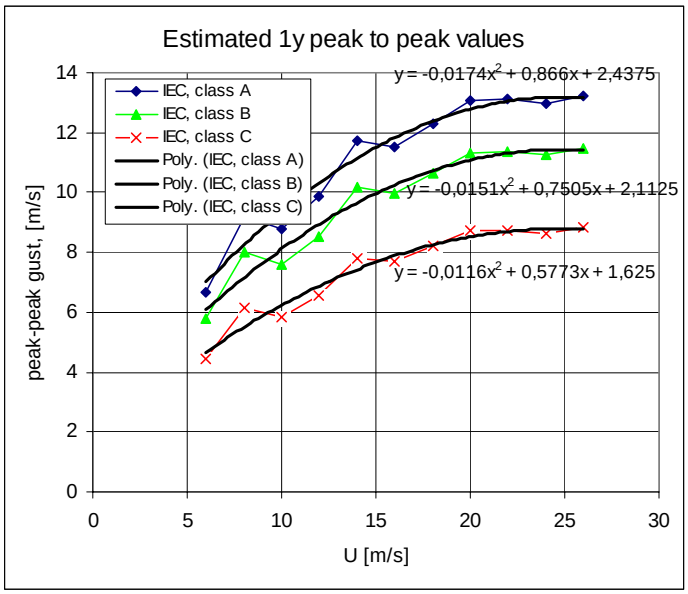

Figure 3: EOG amplitudes for wind turbine class I as function of mean wind speed for turbulence categories A, B and C.

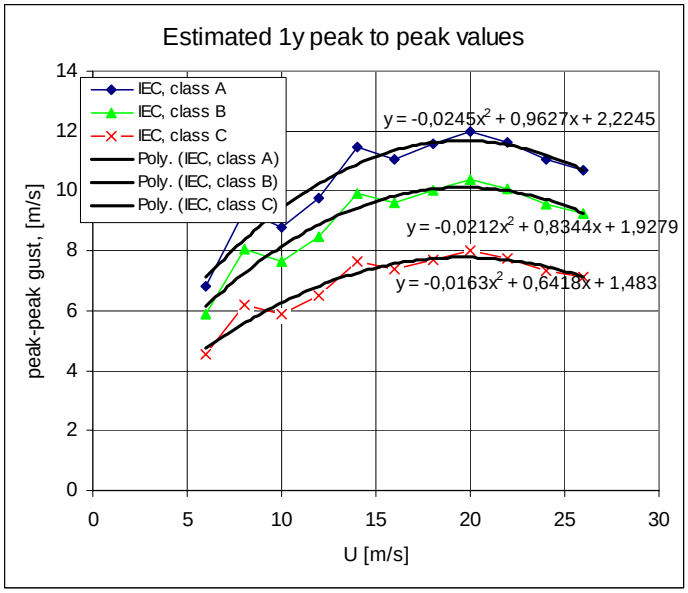

Figure 4: EOG amplitudes for wind turbine class II as function of mean wind speed for turbulence categories A, B and C.

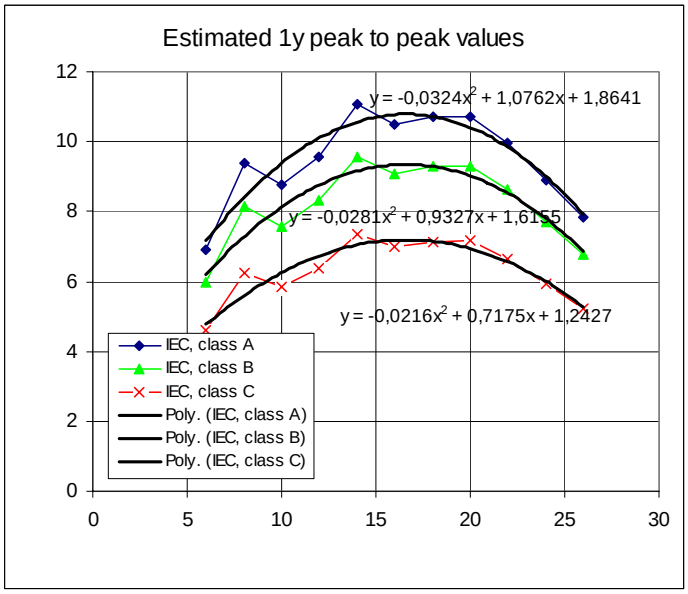

Figure 5: EOG amplitudes for wind turbine class III as function of mean wind speed for turbulence categories A, B and C.

4.2 Recurrence period 50 year

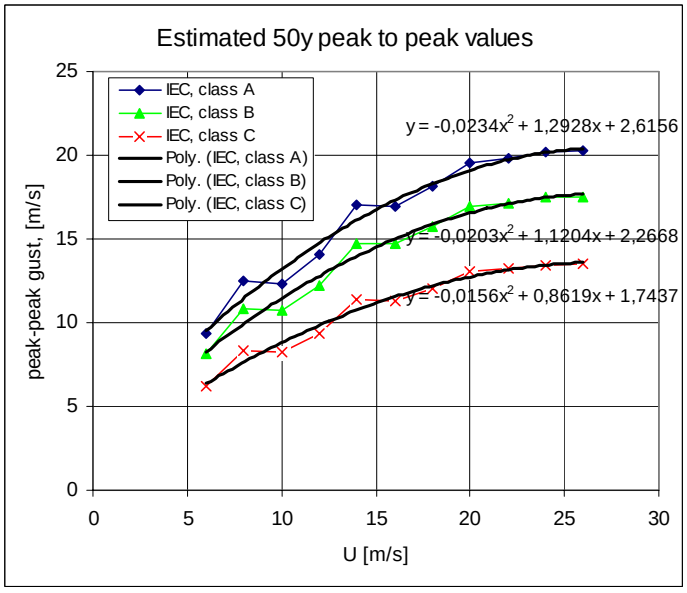

Figure 6: EOG amplitudes for wind turbine class I as function of mean wind speed for turbulence categories A, B and C.

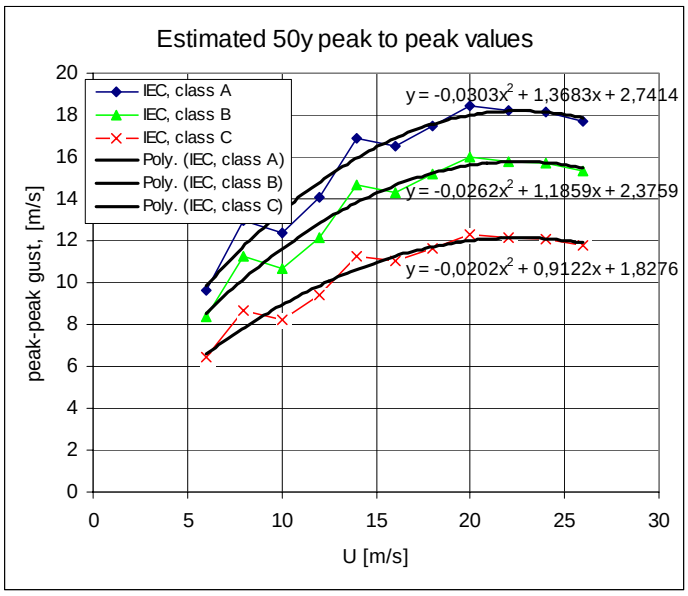

Figure 7: EOG amplitudes for wind turbine class II as function of mean wind speed for turbulence categories A, B and C.

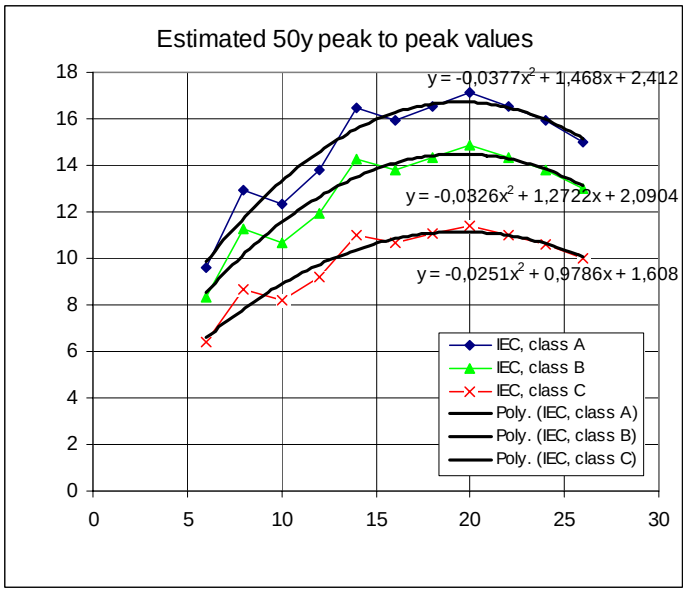

Figure 8: EOG amplitudes for wind turbine class III as function of mean wind speed for turbulence categories A, B and C.

5 DISCUSSION AND SYNTHESIS

The qualitative behaviour of the estimated EOG amplitudes as function of the mean wind speed is characterised by being a single mode function superimposed by (limited) statistical scatter. The maximum of the function reflects the result of two counter acting effects. The first effect is the positive correlation between the size of EOG amplitudes and the wind speed standard deviation. The second effect is the negative correlation between the size of huge wind speed standard deviations and the likelihood of those (i.e. the likelihood of huge mean wind speeds). As a consequence, the maximum is seen both to increase and to shift towards larger mean wind speeds with increasing annual mean wind speed associated with a wind

turbine class (WTC). Obviously, also characteristic is that the estimated EOG amplitudes tend to decrease with decreasing turbulence intensity reflected by the analysed 3 turbulence categories.

To fit the IEC-61400 code framework, the estimated EOG amplitudes have been parameterised by fitting these to a second order polynomial as shown in Figures 3-8.
The fit expressions shown in the figures above can be summarized into the following simple expression:

$$A_{P-P} = I_{15}\left(a\overline{U}^2 + b\overline{U} + c\right), \tag{3}$$

where A_{15} denotes the EOG peak-peak value, $\overline{U}$ is the (10-minute) mean wind speed, I_{15} is the expected value of the turbulence intensity at 15m/s. The coefficients *a*, *b* and *c* depends on the recurrence period.

For a 1-year recurrence period, the coefficients are given in Table 1 below.

WTC	*a*	*b*	*c*
I	-0.116	5.8	16.
II	-0.163	6.4	15.
III	-0.216	7.2	12.

Table 1: EOG amplitude coefficients associated with a 1-year recurrence period.

For a 50-year recurrence period the coefficients are given in Table 2 below.

WTC	*a*	*b*	*c*
I	-0.156	8.6	17.4
II	-0.2	9.1	18.
III	-0.25	9.8	16.

Table 2: EOG amplitude coefficients associated with a 50-year recurrence period.

6 CONCLUSION

Based on the results from a recent analysis of wind speed time series, using wavelet filtering combined with extreme statistics, the *most likely* extreme amplitudes of wind speed gusts, corresponding to the EOG load case in the IEC-61400 code, have been estimated.

The estimation has been performed for recurrence periods 1 year and 50 years, respectively, and for each of the 3 wind speed classes, defined in the IEC-61400 code, the estimated EOG amplitudes have been synthesized into simple algebraic expressions in terms of variables already used in the code.

ACKNOWLEDGEMENT

The Danish Energy Agency funded the present work under the contract ENS 1363/02-0013.

7 REFERENCES

[1] Larsen, G.C., Hansen, K.S. and Pedersen, B.J. (2002). Constrained Simulation of Critical Wind Speed Gusts by means of Wavelets. 2002 Global Wind power Conference and Exhibition, 2-5 April, Paris, France.
[2] IEC 61400-1 Wind Turbine Safety System: part 1, Safety Requirements.
[3] Bierbooms, W., Cheng, P.W., Larsen, G.C. and Pedersen, B.J. (2000). Modelling of Extreme Gusts for Design calculations - NewGust. Publishable Final Report, TU Delft, Delft, The Netherlands.
[4] Database on Wind Characteristics. http://www.winddata.com/.
[5] Larsen, G.C., Pedersen, B.J. and Hansen, K.S.. Extreme coherent wind speed gusts. To appear.

4.4 Analysis of extreme wind shear events

Kurt S. Hansen[1], Gunner Chr. Larsen[2] and Bo Juul Pedersen[3]
[1] Department of Mechanical Engineering, Technical University of Denmark, DK-2800 Lyngby; E-mail:ksh@mek.dtu.dk
[2] Risø National Laboratories, Wind Energy Department, P.O.48, DK-4000 Roskilde; E-mail: gunner.larsen@risoe.dk
[3] NEG-Micon A/S, Alsvej 21, DK-8900 Randers, Denmark; E-mail: bjp@neg-micon.dk

ABSTRACT: In order to continue cost-optimization of modern large wind turbines it is important to continuously increase the knowledge on wind field parameters relevant to design loads. This paper seeks to evaluate requirements, as given in the IEC 61400-1 code, for short-term extreme wind shear relevant for ultimate loading. The evaluation is based on wind speed measurements extracted from the "Database on Wind Characteristics" (www.winddata.com). Distributions for wind shear with short averaging time are estimated. Further, methods for extrapolation of the wind shear profiles to heights up to and above 100m are specified and evaluated.

Keywords: Extreme Wind Conditions, Statistical Analysis, Turbulence, Wind loading, Wind shear.

1 INTRODUCTION

The purpose of this investigation is to evaluate the extreme shear values recommended by the IEC 61400-1 code [1] against measured extreme shear values. The evaluation is based on wind speed measurements recorded at large heights above the terrain (>40m) and restricted to wind speeds $V_{h=10}$ > 10 m/s. Further, the selected measurements represent characteristic vertical spacings for wind turbine load applications. The measurements are extracted from the "Database on Wind Characteristics" [2]. The time series are sampled with a frequency of 1 Hz or more, which enable an estimation of short-term extreme values (T≥2 seconds).

Three different characteristic vertical spacings have been considered, corresponding to three typical wind turbine classes: 1) small rotors (h=40m, D=40m, 5-800kW), 2) medium rotors (h=60m, D=60-80m, 1000-2000kW) and 3) large rotors (h>80m, D>80, 2-5MW).

2 METHODOLOGY

The occurrence of shear, with a limited time scale, within the wind speed recordings is a result of the stochastic nature of the turbulence. The average shear is determined by the terrain roughness and the atmospheric stability whereas the short-term extreme shear is closely related to the turbulence.

2.1 Shear definition

The vertical wind shear, s, is defined as the vertical (mean) wind speed difference (ΔV_T) divided by the vertical distance (Δh):

$$s = \frac{\Delta V_T}{\Delta h} \quad , \tag{1}$$

where

$$\Delta V_T = V_{1T} - V_{2T} \quad \text{and} \quad \Delta h = h_1 - h_2 \ . \tag{2}$$

In equation (2), V_{1T} denotes the mean wind speed (associated with averaging time T) at height h_1, and V_{2T} denotes the mean wind speed (associated with averaging time T) at height h_2. The definition is illustrated in Figure 1. The hub mean wind speed, with reference to the averaging period T, is introduced as

$$V_{hT} = (V_{1T} + V_{2T})/2 \ . \tag{3}$$

2.2 Distributions

Based on wind speed measurements from two different heights we consider N timeseries of vertical wind shear value samples each of size n (which is typically the number of shear estimates within a record time span nT).

An extreme value distribution can be established based on the largest value taken from each sample. The distribution of the largest value among N time series must asymptotically approach the distribution of the largest value within samples of size n, provided that an asymptotic distribution exists. An extreme value distribution, EV1, satisfying these requirements can be derived [4], and initially we will *assume* that the observed extremes can be described by an EV1 distribution.

The shear extremes, conditioned on the hub mean wind speed, will thus be distributed according to a cumulative probability density (CDF) function with two parameters (α,β):

$$F\ (s;\alpha,\beta|V_{hT}) = \exp(-(\exp(-\alpha(s-\beta)) \ . \tag{4}$$

The associated probability density function (PDF), is given by:

$$f\left(s;\alpha,\beta|V_{hT}\right) = \alpha \exp(-\exp(-\alpha(s-\beta)))\exp(-\alpha(s-\beta)) \ . \tag{5}$$

Due to lack of high wind speed measurements, the above conditional distribution will, in the succeeding analysis, be based on only one mean wind speed bin ranging from 12 m/s to a normal wind turbine cut-out wind speed (25m/s).

Having estimated the EV1 distribution, corresponding to a return period Y, the extrapolation to an (arbitrary) a return period pY, are performed based on an independence assumption in a binomial process. The resulting modified extreme value distribution F_p, is thus determined from

$$F_p(\alpha,\beta) = [F(\alpha,\beta)]^p \ . \tag{6}$$

The extreme value with a return period equal to pY is the extreme value that *in average* is exceeded only once during the time span pY, thus corresponding to the (1-1/p) quantile in the extreme value distribution F expressed in equation (4). It can be shown that, for the EV1 distribution, the (1-1/p) quantile in F corresponds (for large p) to the mode (i.e. the most likely extreme value) in the F_p distribution.

The value of p is related to a distribution conditioned on the mean wind speed. Usually, p is determined by initially selecting a return period corresponding to the overall wind climate on the site - i.e. typically the number of years to be considered. Based on knowledge to the mean wind climate on the site p is easily computed for selected mean wind speed bins.

The mean wind speed is conventionally *assumed* to follow a (two parameter) Weibull distribution given by the following CDF and PDF, respectively:

$$F_U(U;k,\beta_U) = 1-\exp\left[-\left(\frac{U}{\beta_U}\right)^k\right] \;;\; U \geq 0 \,,$$

$$f_U(U;k,\beta_U) = \frac{k}{\beta_U}\left(\frac{U}{\beta_U}\right)^{k-1}\exp\left[-\left(\frac{U}{\beta_U}\right)^k\right] \;;\; U \geq 0 \,, \tag{7}$$

where U denotes the mean wind speed, and k, β_U are the (shape and intensity) distribution parameters, respectively.

3 DATA MATERIAL

The present analysis is based on wind speeds measured at observation heights above 40 m from 3 different sites, c.f. Table 1. Furthermore, the investigation is restricted to wind speeds $V_{h=10} > 10$ m/s.

site	Cab	Cab	Cab	Näs	Näs	Ski	Ski
h_1	200	140	80	118	78	101	72
h_2	40	40	40	40	40	41	41
h	120	90	60	79	59	71	57
D	160	100	40	78	40	60	31
V_{hT}>	14.2	13.6	12.9	13.4	12.8	13.2	12.8
TI%	10.3	10.9	11.8	7.6	8.5	7.8	8.1
Freq	2Hz	2Hz	2Hz	1Hz	1Hz	1Hz	1Hz
hour	89	96	90	555	487	402	3080

Table 1: **Available measurements.**

In Table 1, h denotes an artificial hub height equal to $(h_1+ h_2)/2$, D is an artificial rotor diameter equal to Δh, and $V_{hT} > V_h$ where V_{hT} is the characteristic mean wind speed across the artificial rotor disc (3) and V_h is given by

$$V_h = V_{h=10}\left(\frac{h}{10}\right)^{0.14} . \tag{8}$$

3.1 Site description.

The meteorological mast at Cabauw (Cab), NL, which includes measurements at levels up to 200m above ground level, is located in a flat, pastoral terrain. The annual average wind speed, $V_{h=10}$, equals 4.8 m/s.

The meteorological mast at Näsudden (Näs), SE, which includes measurements at levels up to 118m above ground level, is located on Gotland in a flat, coastal terrain. The annual average wind speed, $V_{h=75}$, is 7.9 m/s according to [3].

The meteorological mast at Skipheya (Ski), NO, which includes measurements at levels up to 101m above ground level, is located in a flat, coastal terrain on Frøya. The annual average wind speed, $V_{h=71}$, is 8.8 m/s.

4 RESULTS

The extreme shear values occurring during wind turbine operation are calculated according to the IEC standard [1] for each of the 7 analyzed fictitious wind turbine configurations (c.f. Table 1). The maximum wind speed at hub height is equal to the normal wind turbine cut-out wind speed of 25 m/s. All the measured extreme values are determined for an averaging period T = 2 seconds, corresponding to the IEC peak value[7]. An example of identified minimum and maximum shear values referring to T=2 sec. for configuration #4 is shown on Figure 2a. Figure 2b shows part of the estimated EV1 distribution including a linear. Each data point presented on the figures 2a and 2b represents 600 seconds of measurements. Configuration #4 refers to values recorded at Näsudden with h_1=78m and h_2=40m, respectively.

The extreme distributions, based on the 7 different configurations, are shown in Figure 3. In the succeeding subsections are listed the extracted minimum and maximum extreme shear value, corresponding to a return period of 50 years, for each of the 7 configurations. In addition the corresponding IEC recommended values are specified.

4.1 Small vertical distance

Table 2 shows the estimated IEC and the measured 50-year extreme shear values for vertical distances ranging between 32m and 40 m.

Site/h/D	IEC V_h=25 m/s	Measured min/max
Cabauw/60/40	0.50	-0.27/0.55
Näsudden/59/40	0.57	-0.38/0.47
Skipheya/57/32	0.59	-0.28/0.54

Table 2: Extreme wind shear, T=2 seconds, D=40m, corresponding to a return period of 50 years.

Based on the *Näsudden* measurements, extreme negative shear values equal to –0.38 m/s/m has been estimated which, over the fictitious rotor add up to 15.2 m/s. The estimated extreme positive shear value is 0.47 m/s/m corresponding to 18.8 m/s across the rotor disc.

4.2 Medium vertical distance

Table 3 shows the estimated IEC and the measured 50-year extreme shear values for vertical distances ranging between 60m and 100 m.

[7] The IEC shear value is based on a cosine expression with a period of 12 seconds and WTGS Class A.

Site/h/D	IEC V_h=25 m/s	Measured min/max
Cabauw/90/100	0.26	-0.22/0.26
Näsudden/79/78	0.31	-0.22/0.36
Skipheya/71/60	0.37	-0.17/0.37

Table 3: Extreme wind shear, T=2 seconds, D=60-100m, corresponding to a return period of 50 years.

Table 3 shows, that the IEC standard under-estimates the vertical wind shear at Nasudden site, while the IEC standard agrees to the estimates for the other two sites.

4.3 Large vertical distance

Table 4 shows the estimated IEC and the measured 50-year extreme shear values for a vertical distance equal to 160m.

Site/h/D	IEC V_h=25 m/s	Measured min/max
Cabauw/120/160	0.18	-0.18/0.16

Table 4: Extreme wind shear, V> 14.2 m/s, T=2seconds, D > 100m, corresponding to a return period of 50 years.

Based on 89 hours of measurements, covering very large vertical distances, it seems that the standard corresponds well to the estimated extreme value for this type of terrain.

5 DISCUSSION

The estimated positive extreme shear values agree well with the recommended values in general. However, the IEC standard includes only information on *positive* shear values. The absence of the negative shear in the IEC code does not indicate that it is negligible - resulting negative extreme wind speed differences between -10m/s and -25 m/s (depending the vertical distance) has been observed in the present study.

The estimated extreme distribution parameter values (α,β) for the positive shear values as a function of the observation (hub) height has been fitted to a polynomial expression. Figures 4a and 4b show the parameters as function of the height and the corresponding fit of these values. The performed fit is summarized in:

$$\begin{aligned} \alpha &= 0.007h^3 + 0.0578h + 4.3 \\ \beta &= 2\times10^{-5}h^2 - 0.0047h + 0.36 \end{aligned} \qquad (9)$$

Equation (9) is validated for h ranging between 60m and 120 m. The translation parameter β, c.f. Figure 4b, shows more scattering than scale parameter α, Figure 4a. A sensitivity analysis based on (9) and an increasing rotor size results in an extreme wind speed difference estimate of $\Delta V = 23 \pm 1$ m/s with a return period of 50 years.

The extreme distribution parameter values (α,β) for the negative shear values cannot be used for an extrapolation, as these values show a high degree of scatter.

The estimated extreme shear values can only indicative be compared with those proposed by the IEC 61400-1 code. This is due to the lack of information on the horizontal coherence of the shear. Recall that extreme shear in the IEC is assumed fully coherent over the rotor disk. However, it is not believed that e.g. definition of a wind shear admittance filter function to describe or estimate the shear over the entire rotor disk will alter present results much. This subject will be addressed in future work.

Another important task is to establish relations between shear extreme distributions associated with different averaging times.

6 CONCLUSION

Measurements from coastal and pastoral terrain agree rather well with the IEC recommended extreme shear values. The negative shear extremes ranges between 50% and 100% of the positive extreme shear values. This is recommended to be included in the IEC code in the future.

An empirical equation for the positive, extreme shear as function of hub height has been established. This equation has only been validated against measurements from 3 different sites and heights ranging between 60m and 120 m.

7 REFERENCES

[1] IEC 61400-1, Wind turbine generator systems- Part 1: Safety requirements.
[2] Database on Wind Characteristics, Internet database containing wind field measurements, URL=http://www.winddata.com/.
[3] WEGA II Large wind turbine scientific evaluation report, Final report, Contract No. JOU2-CT93-0349, 2000
[4] Gumbel, E.J.; Statistics of Extremes (1966). Columbia University Express.

8 ACKNOWLEDGEMENTS

This analysis has benefited from measurements downloaded from "Database of Wind Characteristics" located at DTU, Denmark ("http://www.winddata.com/"). Wind field time series from the following sites has been applied: Cabauw (Royal Netherlands Meteorogical Institute, KNMI), Näsudden (Dept. of Meteorology, Uppsala University) and Skipheia (Norwegian University of Science and Technology, Norway).

EU has funded the Database on Wind Characteristics, and the operation and maintenance is funded by IEA R&D Wind, Annex XVII.

9 FIGURES

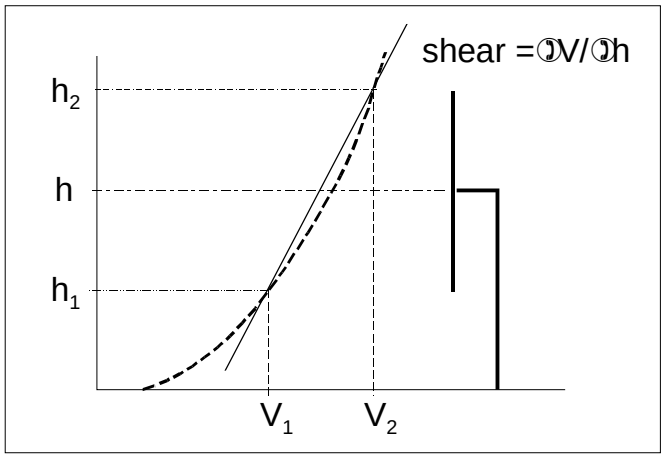

Figure 1: Definition of shear.

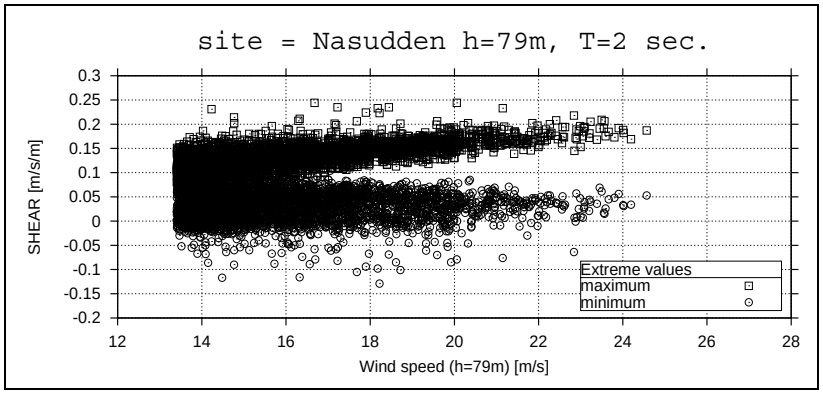

Figure 2a: Example of minimum and maximum shear values.

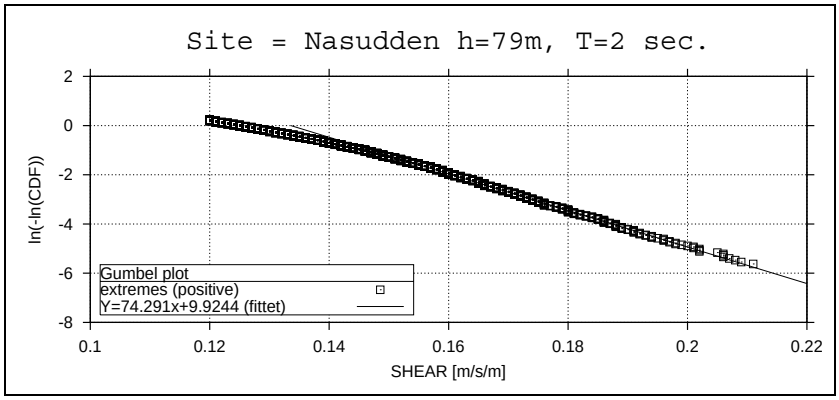

Figure 2b: Gumbel fit of positive shear values.

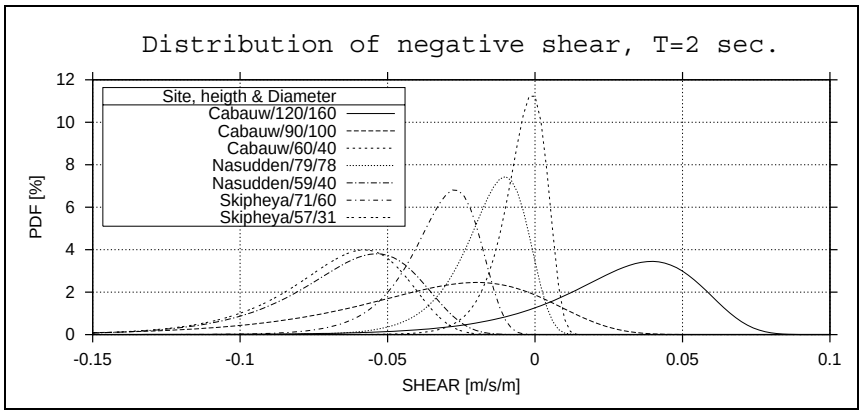

Figure 3a : Distribution of negative shear values.

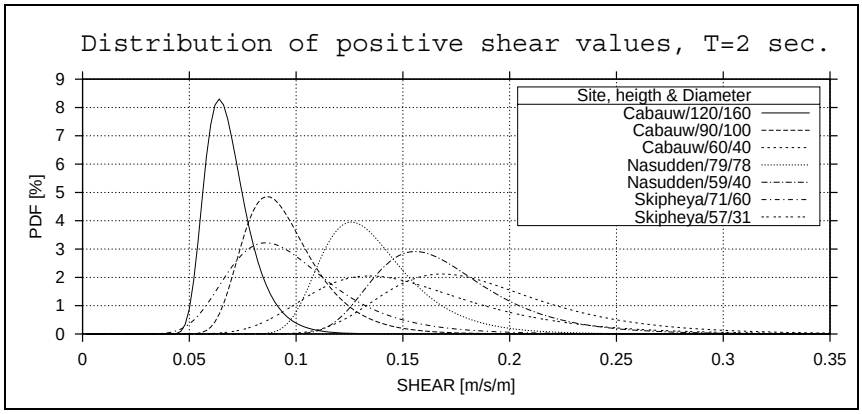

Figure 3b : Distribution of positive shear values.

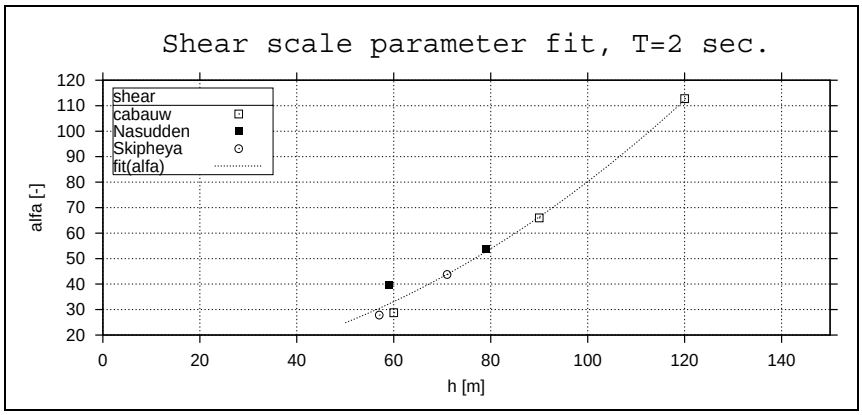

Figure 4a: Scale parameter "alfa", with reference to "positive" extremes.

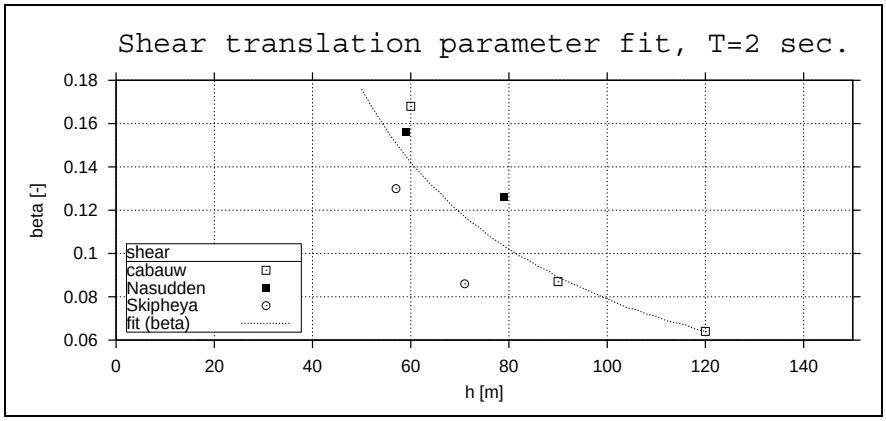

Figure 4b: Fit of "beta" parameters, with reference to "positive" extremes.

4.5 Wind shear extremes at possible offshore wind turbine locations

Kurt S. Hansen[1] and Gunner Chr. Larsen[2]

[1] Department of Mechanical Engineering, Technical University of Denmark,
DK-2800 Lyngby; E-mail <ksh@mek.dtu.dk>
[2] Risø National Laboratories, Wind Energy Department, P.O.48,
DK-4000 Roskilde; E-mail <gunner.larsen@risoe.dk>

ABSTRACT: Positive and negative short-term extreme wind shear distributions (conditioned on the mean wind speed) are determined and compared for a number of offshore sites. The analysis is based on rapidly sampled field measurements (1 - 8 Hz) extracted from the "Database on Wind Characteristics" (www.winddata.com).
Three different averaging periods (2, 5 and 10 seconds) are considered, and for each averaging period a relation between the resulting extreme shear distributions and the averaging time are presented. The short-term extreme shear analysis is based on different spatial distances, and extrapolation to a spatial distance of 100 m has been investigated. Such distances are appropriate for the next generation of offshore wind turbines.
The paper concludes with an estimation of the short-term extreme shear values, which are compared to the values specified in the IEC-61400 code. The extreme IEC shear values seems to be rather conservative for an offshore location, compared to the estimated values based on measurements.

Keywords: Wind shear, offshore, extreme wind conditions, statistical analysis, turbulence, wind loading.

1 INTRODUCTION

This investigation analyses extreme wind shear at offshore locations in the northern Europe, where standard offshore wind turbines with large rotor diameters may be considered. The estimated extreme values are based on measurements extracted from fast sampled time-series (≥ 1 Hz) stored in an Internet wind-database [1]. Each 10-minute period is represented with a minimum and a maximum wind shear observation. Finally, the estimated extreme values are compared with the recommended values based on the IEC code [2, 6].

2 METHODOLOGY

Average offshore wind shear is determined by wave height and the atmospheric stability, whereas short-term extreme shear is closely related to the turbulence. Therefore, the occurrence of shear having a limited time scale and appearing within the wind speed recordings, is a result of the stochastic nature of the turbulence.

2.1 Shear definition

The vertical wind shear gradient, s, is defined as the vertical (mean) wind speed difference (ΔV_T) divided by the vertical distance (Δh):

$$s = \frac{\Delta V_T}{\Delta h} \qquad (1)$$

where

$$\Delta V_T = V_{2T} - V_{1T}$$

and (2)

$$\Delta h = h2 - h1$$

In equation (2), V_{1T} denotes the mean wind speed (associated with averaging time T) at height h_1, and V_{2T} denotes the mean wind speed (associated with averaging time T at height h_2. The definition is illustrated in Figure 1.

The hub mean wind speed, with reference to a 10-minute averaging period, is introduced as

$$V_h = (V_1 + V_2)/2 \ . \quad (3)$$

2.2 Distributions

Based on wind speed measurements from two different heights, we consider N time series of vertical wind shear value samples, each of size n (which is typically the number of shear estimates within a record time span T).

An extreme value distribution can be established based on the largest value taken from each sample. The distribution of the largest value among N time series must approach asymptotically the distribution of the largest value with a time span T, provided that an asymptotic distribution exists. An extreme value distribution, EV1, satisfying these requirements can be derived [4], and initially we will *assume* that the observed extremes can be described by an EV1 distribution.

The shear extremes, conditioned on the hub mean wind speed, will thus be distributed according to a cumulative probability density (CDF) function with two parameters (α,β) as:

$$F\ (s;\alpha,\beta|V_{hT}) = \exp(-(\exp(-\alpha(s-\beta)) \quad (4)$$

The associated probability density function (PDF) is given by:

$$f\left(s;\alpha,\beta|V_{hT}\right) = \alpha \exp(-\exp(-\alpha(s-\beta)))\exp(-\alpha(s-\beta)) \quad (5)$$

The conditional distribution will, in the succeeding analysis, be based on a number of mean wind speed bins, ranging from 8 to 20 m/s.

Having estimated the EV1 distribution corresponding to a return period Y, the extrapolation to an (arbitrary) return period pY, is performed. This is based on an independence assumption in a binomial process. The resulting modified extreme value distribution F_p, is thus determined from

$$F_p(\alpha,\beta) = [F(\alpha,\beta)]^p \quad (6)$$

The extreme value with a return period equal to pY is the extreme value that *in average* is exceeded only once during the time span pY, thus corresponding to the (1-1/p) quantile in the extreme value distribution *F* expressed in equation (4). It can be shown that, for the EV1 distribution, the (1-1/p) quantile in *F* corresponds (for large p) to the mode (i.e. the most likely extreme value) in the F_p distribution.

The value of p is related to a distribution conditioned on the mean wind speed. Usually, p is determined by initially selecting a return period corresponding to the overall wind climate on the site - i.e. typically the number of years to be considered. Based on knowledge of the mean wind climate on the site, p is easily computed for selected mean wind speed bins. The

mean wind speed is conventionally *assumed* to follow a (two parameter) Weibull distribution given by the following CDF and PDF, respectively:

$$F_U(U;k,\beta_U) = 1-\exp\left[-\left(\frac{U}{\beta_U}\right)^k\right] \;;\; U \geq 0 \,, \tag{7}$$

$$f_U(U;k,\beta_U) = \frac{k}{\beta_U}\left(\frac{U}{\beta_U}\right)^{k-1}\exp\left[-\left(\frac{U}{\beta_U}\right)^k\right] \;;\; U \geq 0 \,, \tag{8}$$

where U denotes the mean wind speed, and where k and β_U are the shape and intensity distribution parameters, respectively.

3 DATA MATERIAL

The analysis is based on wind speed measurements extracted from the "Database on Wind Characteristics" [1]. This database contains a huge amount of wind field measurements representing different kinds of terrain types, including a number of coastal and offshore locations.

Due to a lack of offshore measurements recorded at heights above 50 m, we have included some near-coastal wind speed measurements, recorded in offshore sectors. The analysis is based on wind speeds measured at observation heights between 10 and 118 meters above sea level at 3 coastal sites and 5 offshore sites, c.f. Table 1. In Table 1, h denotes an artificial hub height equal to $(h_1+ h_2)/2$, and D is an artificial rotor diameter $\Delta h= h_2- h_1$

3.1 Site descriptions

The configurations used in the analysis are listed in Table 1. Site descriptions are:

i) The meteorological mast at Näsudden, SE, which includes measurements at heights up to 118 m above ground level, is located on Gotland in a flat, coastal terrain.

ii) The meteorological mast at Skipheia (Ski), NO, which includes measurements up to 101 m above ground level, is located in a flat, coastal terrain on Frøya.

iii) The meteorological mast at Lysekil (Lyse) includes measurements up to 65 m above ground level. The mast is located in the Swedish archipelago.

iv) The meteorological masts at Vindeby include measurements up to 48 m above sea level outside a wind farm and are located in the southern part of Denmark.

v) The meteorological mast at Rødsand includes measurements up to 45 m above sea level and it is located offshore in the southern part of Denmark.

vi) The meteorological mast at Gedser Rev (Gedsrev) includes measurements up to 45 m above sea level and it is located offshore in the southern part of Denmark.

vii) The meteorological mast at Middelgrunden (Midgrund) includes measurements up to 45 m above sea level and it is located offshore outside Copenhagen.

viii) The meteorological mast at Horns Rev includes measurements (10 minute averages) up to 62 m above sea level and it is located offshore in the western part of Denmark.

3.2 Determination of distribution parameters.

This section demonstrates how to determine the distribution parameters (α,β) from fast sampled time series, which are used to estimate the 50 years extreme wind shear size.

A Normal Score plot [5] is used to estimate the distributions parameters (α,β). First (a_1,a_2) are determined as a linear regression between the function ln(-ln(cdf)) the shear values s, where a_1 is the slope and a_2 is the intersection with zero. The relation between (a_1,a_2) and (α,β) is given in equation (9) according to [5].

$$\alpha = -a_1 \qquad \beta = -a_2 / a_1 \quad . \tag{9}$$

The example is based on 1294 hours of time series recorded at Näsudden, at level 118 m and 40 m above ground level, respectively. Only observations recorded in an offshore direction, representing the wind speed interval 5 - 25 m/s, are used. The derived 1 Hz wind speed difference signal, with a period of 600 sec, is averaged with a "moving window" technique. The minimum and maximum values, associated with window sizes T=2, 5 and 10 second, are registered. The analysis results in 7765 pairs of minimum and maximum values, as illustrated in Figure 2 with a moving window size equal to T=5 seconds.

The average maximum shear value increases with wind speed, although the overall maximum value is recorded at 18.5 m/s according to Figure 2 for the present Näsudden measurements. The minimum shear value is recorded at low wind speed and for this combination of site and the parameter D/h there is only a limited number of negative wind shear values.

Maximum observed wind shear is 0.21 m/s/m, which equals a positive wind speed difference of 16.4 m/s across a span wise distance of 78 m. The minimum observed wind shear is –0.05 m/s/m equal to a negative wind speed difference of –3.9 m/s.

The extreme values distribution equation (5), based on the maximum values, is fitted from the Normal score plot, Figure 3, for wind speeds in the range 5 – 24 m/s, and an averaging period equal to 5 seconds. The distribution parameters (α,β) are based on (a_1,a_2) according to equation (9). Introducing wind speed bins (ΔV=2 m/s) improves the quality of the distribution parameters as demonstrated on Figure 4, which shows an example of distribution parameters (a_1,a_2) representing minimum, average and maximum observations for different averaging periods T=2, 5 and 10 seconds. The pairs of (a_1,a_2) are grouped in accordance with the binned wind speed V_h (ΔV=2 m/s) and results in a number of distribution parameters as function of wind speed. The distribution parameters (a_1,a_2), as function of wind speed have been estimated for each (D/h)-configuration presented in Table 1.

An example of shear distributions representing V_h>20 m/s is shown on Figure 5. The distributions represents maximum, minimum and average wind shear for averaging periods T=2, 5 and 10 seconds. Note that the "average" distribution is identical to the distributions 10-minute values. Combining shear distributions (equation 5) and the reference wind speed distribution, (equation 7) is used to estimate the extreme value with a desired return period (e.g. 50-year) for this combination.

The estimated 50-year extreme maximum wind speed difference across a 78 m diameter wind turbine at Näsudden for V_h>20 m/s is ΔV_T = 0.295 m/s/m × 78 m = 23.0 m/s for an offshore wind direction (90-300º). This estimate is based on the distribution parameters presented on Figure 4.

4 DATA MATERIAL

4.1 Quantile comparison

With reference to the example above, each combination of distance and height results in a distribution of the (a_1,a_2) coefficients for a number of wind speed bins (Figure 4). The comparison is performed without taking into account the wind climate, and it is limited to the 0.5% quantile shear value at two representative wind speeds, i.e. 15 m/s and 20 m/s. The 0.5% quantiles wind shear values have been calculated for all configurations and are listed in Table 2. While both minimum and maximum shear estimates, s, on Figure 6 fits to logarithmic distributions for h = 80 m and for D = 40 – 80 m, the shear values, s, may be extrapolated up to D = 100 m. The conclusions for large rotors , based on Figure 6, are:

- The short-term minimum wind shear seems to be negligible with increasing distance.
- The short-term maximum wind shear decreases with increasing distance.

The mean wind speed has to be taken into account before the absolute, extreme wind speed difference can be estimated.

Comparing the 0.5 % quantile for both 15 m/s and 20 m/s in Table 2, an increase in the shear value with increasing wind speed is indicated. Unfortunately we do not have sufficient at large wind speeds measurements representing offshore sites to confirm this.

4.2 Extreme 10-min. wind shear observations

The offshore site Horns Rev is located in the north-sea, west of Denmark, but unfortunately only 10 minute statistics and no time series have been recorded. The wind shear distributions for different wind speed bins are shown on Figure 7, and the derived 50-year extreme maximum wind speed difference across a distance of 47 meters, Figure 8, decreases with increasing wind speed, reflecting the change in surface roughness with mean wind speed.

The 50-year extreme estimates for Skipheia, Näsudden and Vindeby show an identical behaviour for the 10 minute wind speed difference, while the short-term estimates increase with increasing wind speed according to Figures 9, 10 and 11.

4.3 Extrapolations

The comprehensive instrumentation at Näsudden results in wind shear gradient, s, distributions for D = 40, 60 and 80 m, each with a reference height h ≈ 80m. The wind shear gradient, s, extrapolations as demonstrated on figure 6, have been used for an extrapolation of 50 years extreme wind speed difference for D = 100 m, as shown in Table 3. The conclusion is that the extreme wind speed difference is unimodal as function of the rotor size with a maximum around D = 60 m for h = 80 m. This does not agree well with the IEC-61400 shear values according to [1], which increases monotonically with increasing rotor size.

4.4 IEC comparisons and recommendations

Extreme wind shear values (EWS) are calculated according to [1] for V_h = 20 m/s and listed in Table 1. The shear values are in the range 14 – 20 m/s for all configurations. Table 3 includes the recommended extreme shear values (EWS) for h = 80m, located offshore. According to this table, EWS underestimates substantially the shear size for small rotors (with large hub heights), while the values converge for increasing rotor diameters (>100m).

5 CONCLUSION

A number of wind shear analyses have been performed on offshore and coastal (offshore direction) time series. The number of time series at large mean wind speeds is limited. The analysis shows that 1) the extreme 50-years shear gradient values, s, decrease with increasing rotor diameters, and 2) the estimated extreme wind speed differences are comparable or (for

small rotors) even larger than the values recommended by the IEC standard. Furthermore, no significant negative wind shear need be included for offshore rotors, and so a wind shear value of zero is recommended as the minimum value with increasing rotor diameters. Increasing the short-term wind shear average period, T, reduces the extreme values.

There is a lack of suitable offshore time series, which are recorded at heights above 50 m and at mean wind speeds more than 20 m/s. More offshore measurements for validation of extreme offshore shear (EWS) are therefore recommended.

6 REFERENCES

[1] Database on Wind Characteristics, Internet wind database of wind field measurements, URL=http://www.winddata.com/.
[2] IEC 61400-1, Wind turbine generator systems- Part 1: Safety requirements.
[3] Programme for measuring wind, wave and current at Horns Rev report, Eltra PSO-2000, Proj.nr. EG-05 3248 (December 2002).
[4] Gumbel, E.J.; Statistics of Extremes (1966). Columbia University Express.
[5] Larsen, G.C, Off-shore fatigue turbulence (2001), Wind Energy, Vol.4, Issue 3, 2001.
[6] Kurt S. Hansen[1] and Gunner Chr. Larsen (2203), Extreme offshore wind shear, Proc. OWEMES, Naples.

7 ACKNOWLEDGEMENTS

This analysis has benefited from measurements downloaded from the internet database: "Database of Wind Characteristics" located at DTU, Denmark. Internet: "http://www.winddata.com/". Wind field time series provided from the following institutes have been used: Dept. of Meteorology, Uppsala University, Norwegian University of Science and Technology (NTNU) Norway, Risø National Laboratories, Eltra and Tech-wise Denmark.

"Database on Wind Characteristics" was originally funded by EU, and currently the operation and maintenance is funded by IEA R&D Wind, Annex XVII.

8 TABLES AND FIGURES

Table 1: Available measurements, including calculated extreme wind shear at V_h=20 m/s for each site.

	Site	D	h	Freq	Hours	EWS
1.1- coastal	Näsudden (SE)	38	59	1 Hz	3813	14.1
1.2- coastal	Näsudden (SE)	58	69	1 Hz	3706	15.9
1.3- coastal	Näsudden (SE)	78	79	1 Hz	3883	17.5
2.1- coastal	Skipheia (NO)	51	46	1 Hz	5040	16.9
2.2- coastal	Skipheia (NO)	60	71	1 Hz	3359	16.0
2.3- coastal	Skipheia (NO)	81	61	1 Hz	3280	19.3
3.1-coastal	Lysekil (SE)	33	49	1 Hz	2227	13.9
3.2- coastal	Lysekil (SE)	41	45	1 Hz	2247	15.4
3.3- coastal	Lysekil (SE)	48	34	1 Hz	2865	18.5
3.4- coastal	Lysekil (SE)	55	38	1 Hz	2821	19.1
4.1 – offshore	Vindeby	33	29	5 Hz	357	16.1
5.1 – offshore	Gedser Rev	35	28	5 Hz	547	16.8
6.1- offshore	Rødsand	35	28	5 Hz	431	16.8
7.1- offshore	Midgrund	35	28	5 Hz	340	16.8
8.1- offshore	Horns Rev	47	39	10 minutes average	7139	17.2

Table 2: 0.5 % quantiles of extreme positive and negative wind shear values, T=2 sec., V_h= 15 & V_h>20 m/s.

site	D	h	V_h=15 m/s		V_h>20 m/s	
			MIN	MAX	MIN	MAX
Näsudden	38	59	-0.090	0.256	-0.100	0.360
Näsudden	58	69	-0.040	0.210	-0.040	0.280
Näsudden	78	79	-0.020	0.200	-0.010	0.230
Näsudden	40	78	-0.050	0.338	-0.080	0.320
Näsudden	60	88	-0.030	0.255	-0.015	0.310
skipheia	60	71	-0.060	0.155	-0.080	0.250
skipheia	81	61	-0.045	0.150	-0.055	0.235
skipheia	51	46	-0.065	0.210	-0.095	0.260
Lysekil	39	30	-0.140	0.265		
Lysekil	48	34	-0.105	0.220		
Lysekil	55	38	-0.090	0.200	-0.110	0.240
Lysekil	34	41	-0.125	0.305	-0.165	0.375
Lysekil	41	45	-0.100	0.260	-0.120	0.335
Vindeby	33	29	-0.090	0.260		
Vindeby	33	29	-0.090	0.245		
Rødsand	40	28	-0.0850	0.285		
Gedsrev	37	26	-0.0650	0.230		
Midgrund	40	30	-0.0750	0.205		

Table 3: Extreme 50-years wind speed difference at Näsudden, h=80 m.

V	D = 40	D = 60	D = 80	D = 100
V_h = 15 m/s	20.3	26.0	25.0	22.2
V_h = 17 m/s	21.1	25.1	24.5	19.0
V_h = 19 m/s	18.4	28.1	23.2	20.0
V_h > 20 m/s	21.4	27.6	24.0	19.6
EWS, z_h=80m	13.6	15.6	17.5	19.5

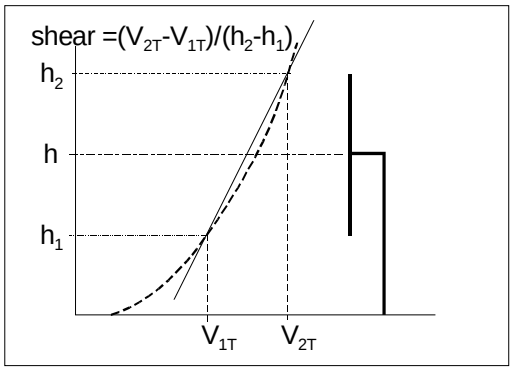

Figure 1: Definition of wind

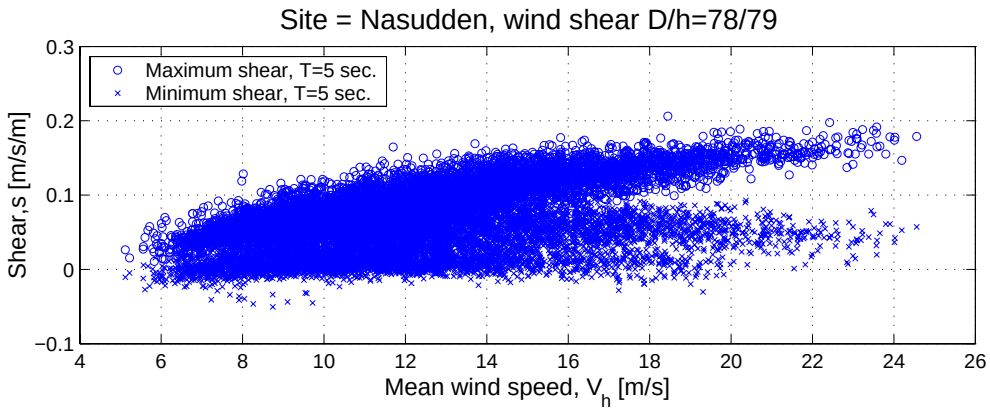

Figure 2: Minimum and maximum wind shear observations at Nasudden; D/h=78/79 m; T= 5 seconds.

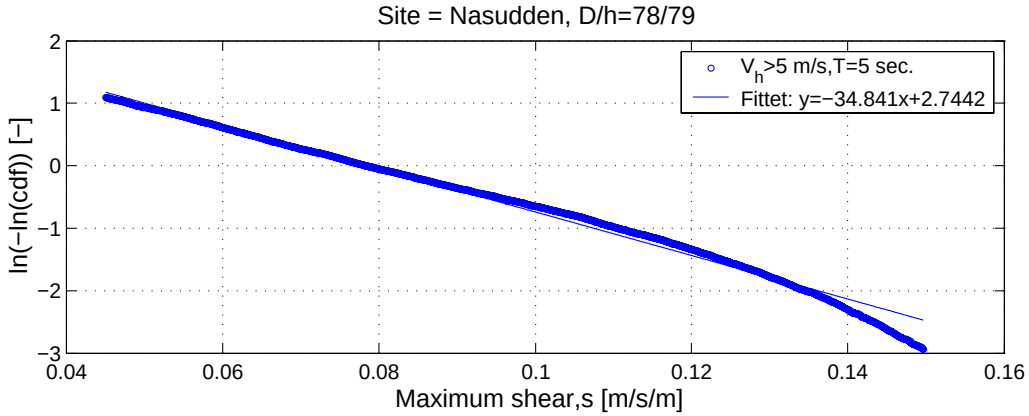

Figure 3: Normal Score plot of positive (MAX) shear values (a_1,a_2) = (-34.841,2.7442).

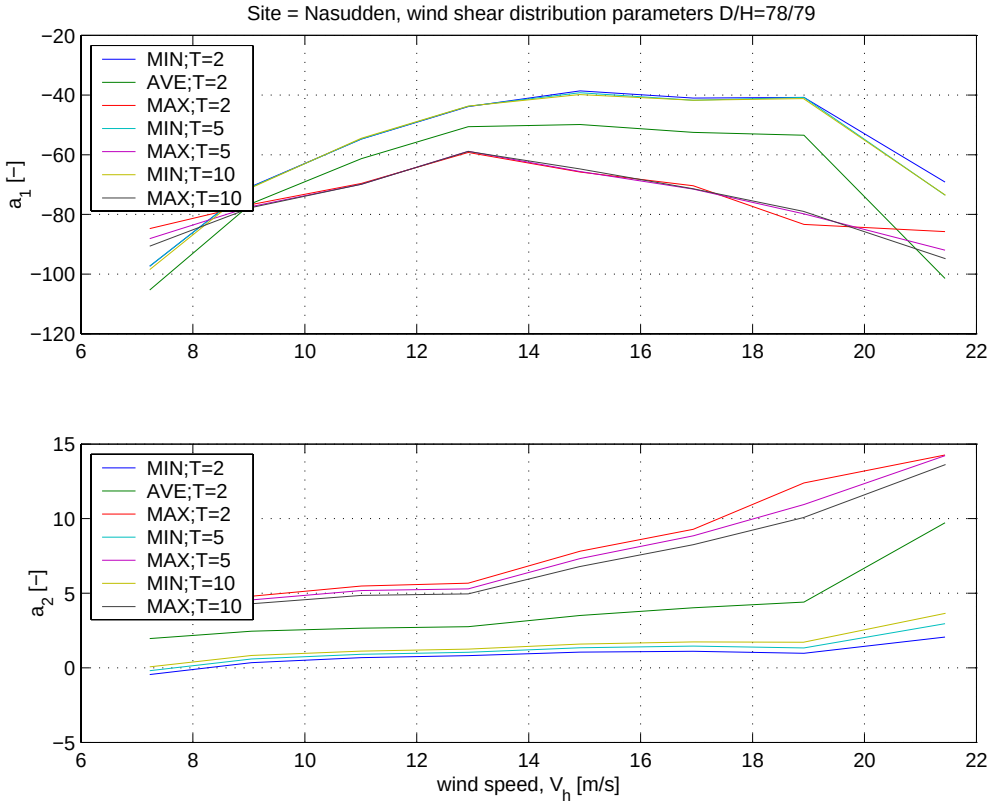

Figure 4: Distributions parameters (a_1,a_2) – as function of wind speed for T= 2, 5 and 10 seconds.

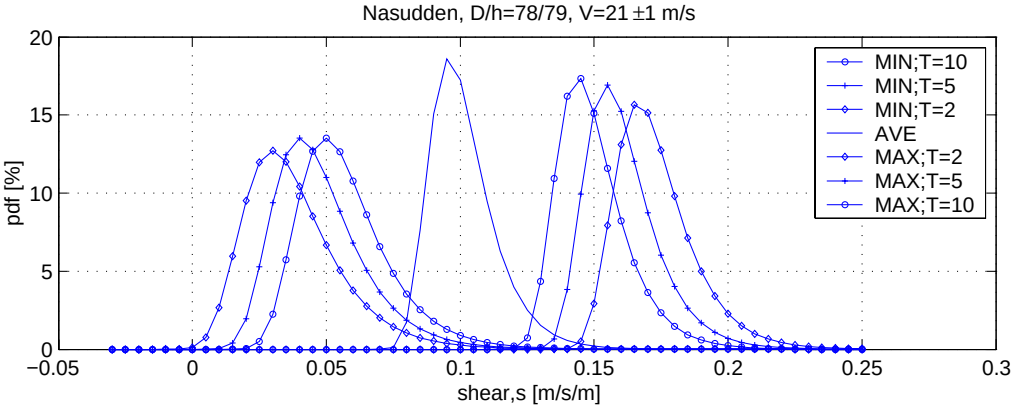

Figure 5: Example of wind shear distributions, (T=2, 5 & 10 seconds), for D/h= 78/79 m and V>20 m/s at Nasudden.

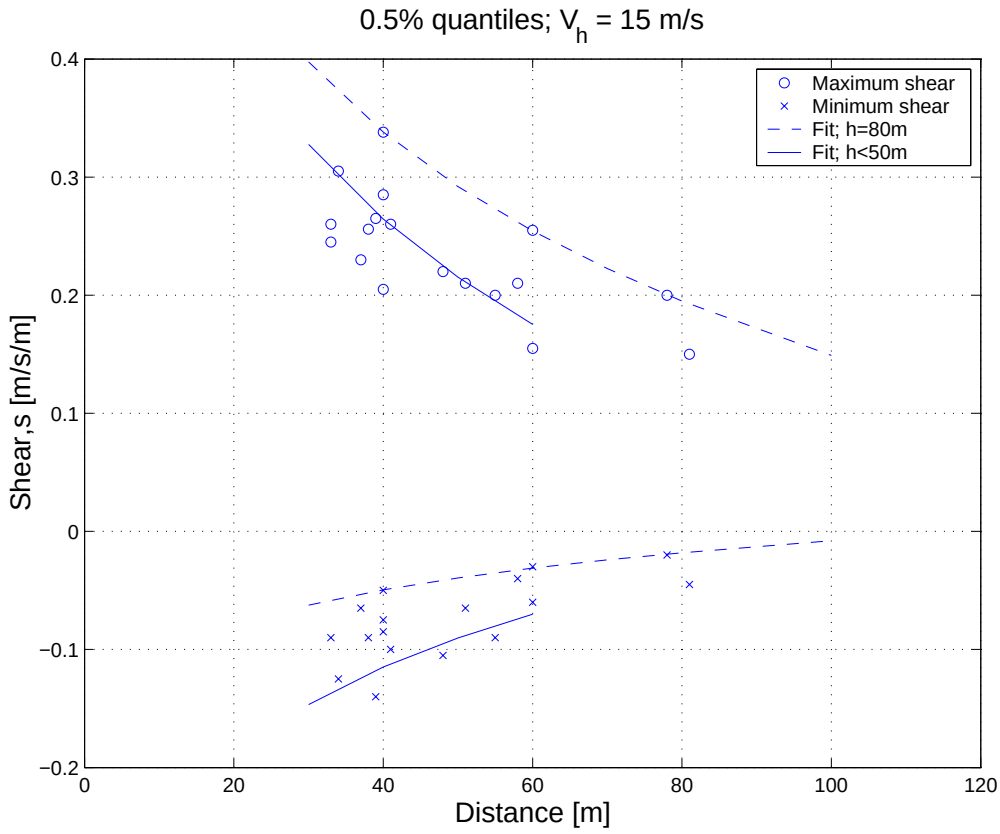

Figure 6: 0.5% quantiles of extreme wind shear observations, T=2 seconds.

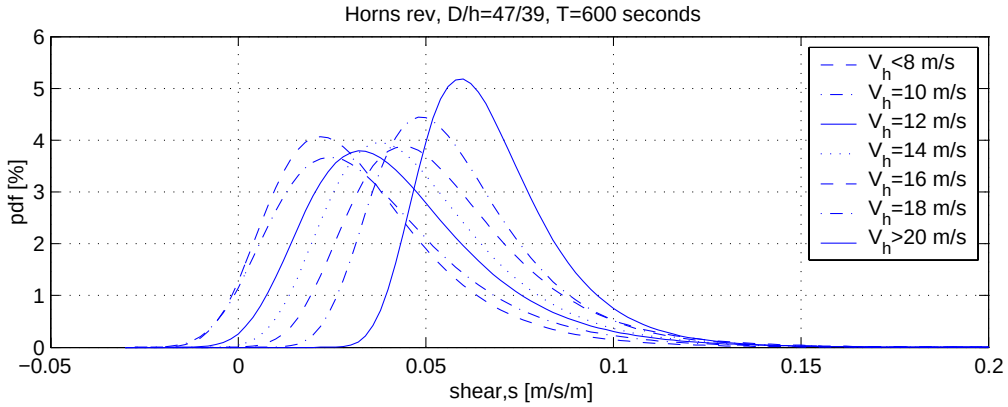

Figure 7: Estimated distributions of wind shear at Horns Rev (D/h=47/39 m), T=600 seconds.

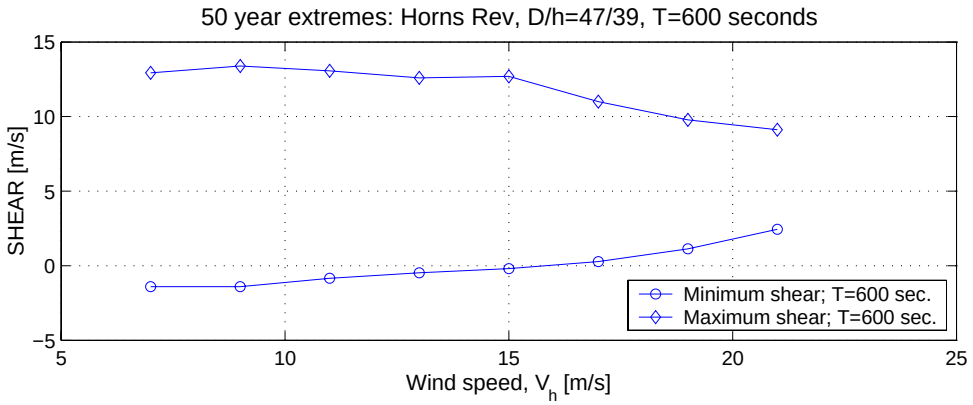

Figure 8: 50-years extreme wind shear at Horns Rev, D/h=47/39, T=600 seconds.

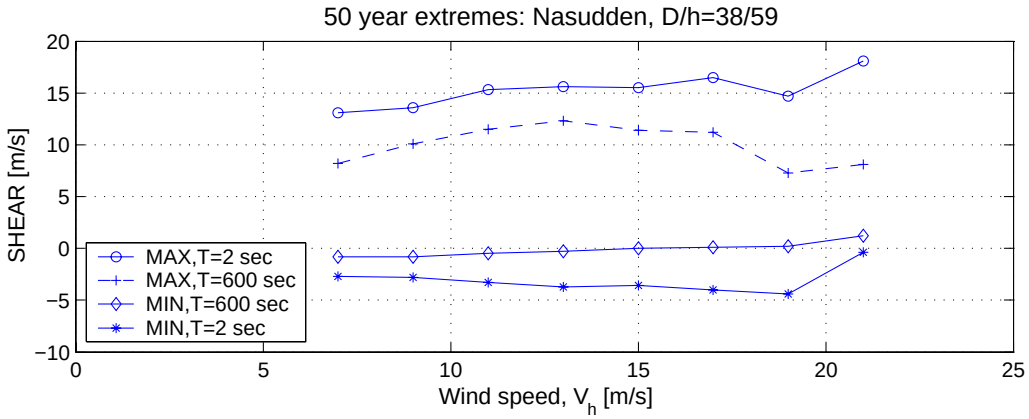

Figure 9: 50-years extreme wind shear at Skipheia, D/h=51/46, T=2, 5 & 10 seconds.

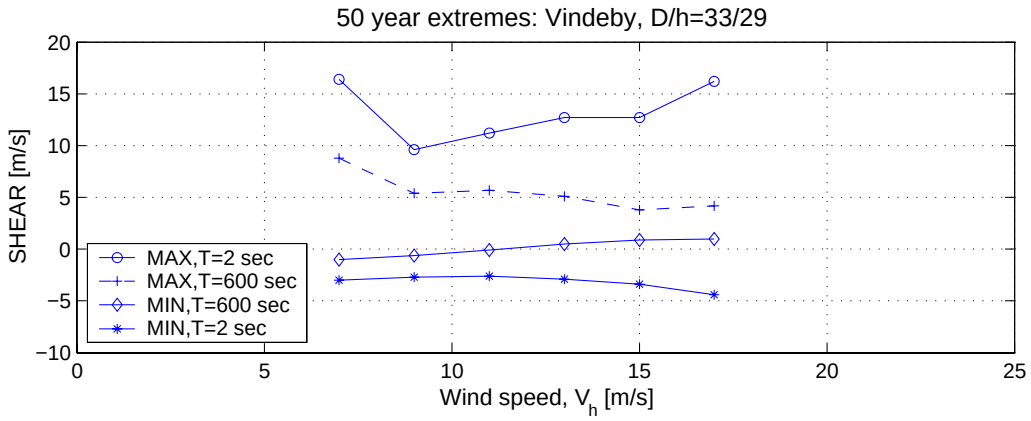

Figure 10: 50-years extreme wind shear at Nasudden, D=h=38/59 m, T=2 & 600 seconds.

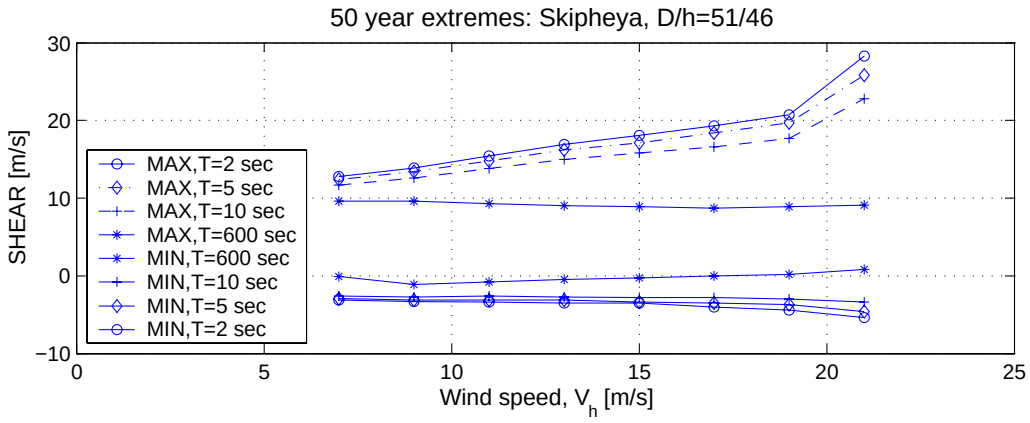

Figure 11: 50-year extremes wind shear at Vindeby, D/h=33/29 m, T=2 & 600 sec.

5 Summary of conclusions

The findings from the selected collection of papers are summarized below. As for the *fatigue loading*, the following can be concluded:

- The analysis performed on *design turbulence intensity* has demonstrated that signal de-trending reduces the mean turbulence intensity with up to 11 % - depending of site characteristics. The turbulence intensity, specified in the IEC code, corresponds to the estimated design turbulence intensity at wind speed below 15 m/s, while IEC values seems to be more conservative for wind speeds above 15 m/s *except at complex sites.*
- The analysis dedicated the spatial coherence of turbulence has resulted in formulation of a new (empirical) coherence model. The model has been demonstrated to fit well with the available data, however, with a slight overestimation of one of the analysed data sets. Predictions from the empirical model have subsequently been compared with predictions from the Mann-model as well as with predictions from the IEC code model. The Mann-model seems to resemble the measured data (and the predictions from new empirical model) better than the IEC-model.

Turning to the investigations of *ultimate loading* can be the following emerges:

- For *extreme wind speed gusts* at offshore locations it has been demonstrated that, although a shallow water site is exposed to larger water surface roughness, the more frequent occurrence of large mean wind speeds at a coastal ocean site more than compensate for the increased roughness on shallow water sites regarding generation of extreme wind speed gusts. The most likely extreme gusts, at the coastal ocean site, exceed the most likely extreme gusts, at the shallow water site, with 16% and 22% (for a one-year and a fifty-year recurrence period), respectively.
- Using a wavelet expansion technique, (coherent) *EOG wind speed gust* events with return periods 1 year and 50 years, respectively, have been estimated based on a large number of one-point measurements. The gust estimates have subsequently been compared with predictions based on the IEC code. For *identical turbulence conditions*, the IEC code tend to somewhat under-predict the estimated extreme gust events, except for the high wind region associated with the return period 1 year.
- Assuming the mean wind speed to be Rayleigh distributed (as specified in the IEC code) and further adopting the conjecture that wind speed gust amplitudes scale directly with the turbulence standard deviation, the *most likely extreme amplitudes* of wind speed gusts, corresponding to the EOG load case in the IEC-61400 code, have been estimated. The estimation has been performed for recurrence periods 1 year and 50 years, respectively. For each of the 3 wind speed classes, defined in the IEC-61400 code, the estimated EOG amplitudes have been synthesized into simple algebraic expressions in terms of variables already used in the code.
- Using conventional extreme statistics, short-term (positive and negative) *shear events* have been analyzed. Estimated most likely positive shear events, based on analyses of measurements from *coastal and pastoral terrain,* agree rather well with the extreme shear values specified in the IEC code. The negative shear extremes ranges between 50% and 100% of the positive extreme shear values. This is recommended to be included in the IEC code in the future.
- *Extreme wind shear* analyses have been performed time series related to *offshore* wind conditions. The analysis shows that the extreme 50-years shear gradient values decrease with increasing rotor diameters, and that the estimated extreme wind speed

differences are comparable or (for small rotors) even larger than the values recommended by the IEC code. Further, no significant extreme negative wind shear event needs be included for offshore rotors. Finally, increasing the short-term wind shear average period, T, reduces the resulting extreme values.

Acknowledgements

The Ministry of Environment and Energy, Danish Energy Agency, The Netherlands Agency for Energy and the Environment (NOVEM), The Norwegian Water Resources and Energy Administration (NVE), The Swedish National Energy Administration (STEM), The Government of the United States of America and the IEA R&D Wind Agreement are all acknowledged for the support that have made the completion of this work possible.

6 References.

[1] Hansen, K.S. and Courtney, M.S. (1999). Database on Wind Characteristics. ET-AFM-9901, Department of Energy Engineering, DTU, Denmark.

[2] Larsen, G.C. and Hansen, K.S. (2001). Database on Wind Characteristics - Philosophy and Structure. Risø-R-1299.

[3] Larsen, G.C. and Hansen, K.S. (2001). Database on Wind Characteristics - Users Manual. Risø-R-1300.

[4] Larsen, G.C. and Hansen, K.S. (2001). Database on Wind Characteristics - Contents of Database Bank. Risø-R-1301 (EN).

[5] Hansen, K.S. and Larsen, G.C. (2003). Parameterisation of Turbulence Intensity. *European Wind Energy Conference,* Madrid, June 16-19.

[6] Larsen, G.C. and Hansen, K.S. (2003). Spatial Coherence of the Longitudinal Turbulence Component (2003). *European Wind Energy Conference,* Madrid, June 16-19.

[7] Larsen, G.C. and Hansen, K.S. (2001). Statistics of Off Shore Wind Speed Gusts. EWEC'01, Copenhagen, Denmark, 2-6 July.

[8] Larsen, G.C., Hansen, K.S. and Pedersen, B.J. (2002). Constrained Simulation of Coherent Wind Speed Gusts by Means of Wavelets. *Global Windpower*, Paris, April 2002.

[9] Larsen, G.C. and Hansen, K.S. (2003). On the Most Likely EOG Amplitudes. *European Wind Energy Conference,* Madrid, June 16-19.

[10] Hansen, K.S., Larsen, G.C. and Pedersen, B.J. (2002). Analysis of Extreme Wind Shear Events. *Global Windpower*, Paris, April 2002.

[11] Hansen, K.S. and Larsen, G.C. (2003): *Wind Shear Extremes at Possible Offshore Wind Turbine Locations.* Wind Eng. (2003) **27**, 339 - 350.

[12] Larsen, G.C. and Hansen, K.S. (2004). Database on Wind Characteristics – Contents of Database Bank – revision I. Risø-R-1472(EN).

Bibliographic Data Sheet **Risø-R-1473(EN)**

Title and authors

DATABASE ON WIND CHARACTERISTICS - Analyses of Wind Turbine Design Loads

Gunner C. Larsen and Kurt S. Hansen

ISBN	ISSN
87-550-3359-8 (Internet)	0106-2840

Department or group	Date
Wind Energy Department	June 2004

Groups own reg. number(s)	Project/contract No(s)
1110024-01	ENS-1363/02-0013

Pages	Tables	Illustrations	References
82	12	51	11

Abstract (max. 2000 characters)

The main objective of IEA R&D Wind Annex XVII - Database on Wind Characteristics - has been to provide wind energy planners, designers and researchers, as well as the international wind engineering community in general, with a source of actual wind field data (time series and resource data) observed in a wide range of different wind climates and terrain types. Connected to an extension of the initial Annex period, the scope for the continuation was widened to include also support to the international wind turbine standardisation efforts.. The project partners are Sweden, Norway, U.S.A., The Netherlands and Denmark, with Denmark as the Operating Agent.

The reporting of the continuation of Annex XVII falls in two separate parts. Part one accounts in details for the available data in the established database bank, and part two describes various data analyses performed with the overall purpose of improving the design load cases with relevance for to wind turbine structures.

The present report constitutes the second part of the Annex XVII reporting. Both fatigue and extreme load aspects are dealt with, however, with the main emphasis on the latter.

The work has been supported by The Ministry of Environment and Energy, Danish Energy Agency, The Netherlands Agency for Energy and the Environment (NOVEM), The Norwegian Water Resources and Energy Administration (NVE), The Swedish National Energy Administration (STEM) and The Government of the United States of America.

Descriptors INIS/EDB
DATA ANALYSIS; FATIGUE; GUSTS; IMPACT STRENGTH; INFORMATION SYSTEMS; SHEAR; STORMS; TIME-SERIES ANALYSIS; TURBULENCE; VELOCITY; WIND; WIND LOADS; WIND TURBINES.